NUSC Technical Report 8887
21 May 1991

(2)

AD-A237 392

Spectra and Covariances for "Classical" Nonlinear Signal Processing Problems Involving Class A Non-Gaussian Noise

Albert H. Nuttall
Surface ASW Directorate

David Middleton
Consultant/Contractor

DTIC
S ELECTE D
JUN 27 1991
B

Naval Underwater Systems Center
Newport, Rhode Island / New London, Connecticut

Approved for public release; distribution is unlimited.

91-03101

91 2 3

PREFACE

This research was conducted under NUSC Project No. A70272, Subproject No. RR0000-N01, **Selected Statistical Problems in Acoustic Signal Processing**, Principal Investigator Dr. Albert H. Nuttall (Code 304). This technical report was prepared with funds provided by the NUSC In-House Independent Research and Independent Exploratory Development Program, sponsored by the Office of the Chief of Naval Research. Also, this research is based in part on work by Dr. David Middleton, supported originally by Code 10 under ONR Contract N00014-84-C-0417 with Code 1111.

The technical reviewer for this report was Roy L. Deavenport (Code 3112).

REVIEWED AND APPROVED: 21 MAY 1991

for

DAVID DENCE

ATD for Surface Antisubmarine Warfare Directorate

REPORT DOCUMENTATION PAGE

Form Approved
OMB No. 0704-0188

Public reporting burden for this collection of information is estimated to average 1 hour per response, including the time for reviewing instructions, searching existing data sources, gathering and maintaining the data needed, and completing and reviewing the collection of information. Send comments regarding this burden estimate or any other aspect of this collection of information, including suggestions for reducing this burden, to Washington Headquarters Services, Directorate for Information Operations and Reports, 1215 Jefferson Davis Highway, Suite 1204, Arlington, VA 22202-4302, and to the Office of Management and Budget, Paperwork Reduction Project (0704-0188), Washington, DC 20503

1. AGENCY USE ONLY *(Leave blank)*

2. REPORT DATE
21 May 1991

3. REPORT TYPE AND DATES COVERED
Progress

4. TITLE AND SUBTITLE
Spectra and Covariances for "Classical" Nonlinear Signal Processing Problems Involving Class A Non-Gaussian Noise

5. FUNDING NUMBERS
PE 61152N

6. AUTHOR(S)
Albert H. Nuttall
David Middleton

7. PERFORMING ORGANIZATION NAME(S) AND ADDRESS(ES)
Naval Underwater Systems Center
New London Laboratory
New London, CT 06320

8. PERFORMING ORGANIZATION REPORT NUMBER
TR 8887

9. SPONSORING/MONITORING AGENCY NAME(S) AND ADDRESS(ES)
Chief of Naval Research
Office of the Chief of Naval Research
Arlington, VA 22217-5000

10. SPONSORING/MONITORING AGENCY REPORT NUMBER

11. SUPPLEMENTARY NOTES

12a. DISTRIBUTION/AVAILABILITY STATEMENT
Approved for public release; distribution is unlimited.

12b. DISTRIBUTION CODE

13. ABSTRACT *(Maximum 200 words)*

Because of the critical rôle of non-Gaussian noise processes in modern signal processing, which usually involves nonlinear operations, it is important to examine the effects of the latter on such noise and the extension to added signal inputs. Here, only non-Gaussian (specifically Class A) noise inputs, with an additive Gaussian component, are considered.

The "classical" problems of zero-memory nonlinear (ZMNL) devices serve to illustrate the approach and to provide a variety of useful output statistical quantities, e.g., mean or "dc" values, mean intensities, covariances, and their associated spectra. Here, Gaussian and non-Gaussian noise <u>fields</u> are introduced, and their respective temporal and spatial outputs are described and numerically evaluated for representative parameters of the noise and the ZMNL devices. Similar

14. SUBJECT TERMS
covariance
nonlinear
non-Gaussian
spectra
Class A noise
signal processing

15. NUMBER OF PAGES

16. PRICE CODE

17. SECURITY CLASSIFICATION OF REPORT	18. SECURITY CLASSIFICATION OF THIS PAGE	19. SECURITY CLASSIFICATION OF ABSTRACT	20. LIMITATION OF ABSTRACT
UNCLASSIFIED	UNCLASSIFIED	UNCLASSIFIED	SAR

13. ABSTRACT (continued)

statistics for carriers which are phase or frequency modulated by Class A (and Gaussian) noise are also presented, numerically evaluated, and illustrated in the figures. A series of appendices and programs provide the technical support for the numerical analysis.

14. SUBJECT TERMS (continued)

zero memory nonlinearity
ν-th law rectification
frequency modulation
phase modulation

TABLE OF CONTENTS

Accession For
NTIS GRA&I ☑
DTIC TAB ☐
Unannounced ☐
Justification
By
Distribution/
Availability Codes
Dist | Avail and/or Special
A-1

LIST OF FIGURES

LIST OF PRINCIPAL SYMBOLS

A	overlap index (A_A) of Class A noise
$\alpha(R,t)$	input (noise) field
B_ν	output covariance function, cf. (2.7a)
b	dimensionless factor, (2.44) et seq.
D_P, D_F	phase- and frequency-modulation scaling factors
δ	(Dirac) delta function
F_1, F_2	characteristic functions
FM	frequency modulation
$f(i\xi)$	Fourier transform of rectifier transfer function
g	ZMNL input-output transfer function
Γ'	σ_G^2/Ω_{2A} = "Gaussian" factor
$H_1^{(\nu)}$	scaling parameter for ν-th law detector outputs, (2.18a,b,c)
J_o	Bessel function of first kind
$K, K_{L,G}$	covariances
k_L, k_G	normalized covariances
ξ, ξ_1, ξ_2	characteristic function variables
$M_y, \hat{M}_y, \hat{M}'_y$	second-moment functions, (2.7), (2.8), (2.11)
$\mu_F, \hat{\mu}_F$	frequency-modulation indexes
$\mu_P, \hat{\mu}_P$	phase-modulation indexes
ν	power law of half-wave rectifier
$\hat{\nu}, \hat{\nu}$	normalized wavenumber, cf. (2.33a)
$\Omega_{G,A}$	covariance functions (angle-modulation), section 2.2-6

Ω_{2A}	intensity of Class A noise
Ω_o	spectral parameter in FM, PM, (2.42c)
PM	phase modulation
$\Delta R, \widehat{\Delta R}$	spatial correlation distances
$\hat{R}$	array operator
Re z	real part of z
ρ	"overlap" correlation function, (2.3)
σ^2_{m+n}	noise variance
σ^2_G	intensity of Gauss noise component
T	observation time
T_s	waveform duration of elementary noise source
τ	t_2-t_1, delay (correlation) time
$\hat{\tau}, \hat{\tau}'$	normalized delay parameters
$w(\hat{\omega})$	normalized intensity spectrum, (2.52)
$W_2, \hat{W}_2$	(wavenumber) intensity spectra
$W_{()}, \hat{W}_{()}$	(frequency) intensity spectra
x, x(t)	array outputs = inputs to ZMNL devices
y, y(t)	outputs of ZMNL devices
Y_a	correlation parameter, cf. (2.7b)
ZMNL	zero-memory nonlinear

LIST OF NORMALIZING AND NORMALIZED PARAMETERS

1. $\hat{\tau} = \beta\tau$; $\beta = 1/\overline{T}_s$; $\tau = t_2 - t_1$: correlation delay
   $\overline{T}_s$ = mean duration of typical interfering signal
2. $\rho = 1-|\hat{\tau}|$ for $|\hat{\tau}| < 1$, zero otherwise; (2.3): "overlap" correlation function
3. $\widehat{\Delta R} = \Delta R/\Delta_L$ (≥ 0); $\Delta R = |R_2 - R_1|$, correlation distance
4. $\hat{\omega} = \omega/\beta = \omega\overline{T}_s$; $\omega = 2\pi f$: normalized (angular) frequency
5. $\Delta\hat{\omega}_L = \Delta\omega_L/\beta$; normalized (frequency) spectrum bandwidth, for Class A noise model
6. $\Delta\hat{\omega}_G = \Delta\omega_G/\beta$; normalized (frequency) spectrum bandwidth, for Gauss noise component
7. Δ_L = rms spread of spatial covariance of non-Gaussian noise field component
8. Δ_G = rms spread of spatial covariance of Gaussian noise field component
9. $\hat{k} = k\Delta_L$: normalized wavenumber
10. $\Delta\omega_N$ = spectrum bandwidth of modulating (RC-Gauss) noise; cf. (2.43) and [1; section 14.1-3]; cf. (11) ff.
11. $\Delta\omega_N \rightarrow \Delta\omega_{N(L)}$ = bandwidth of non-Gaussian component of modulating noise in PM and FM;
    $\Delta\omega_N \rightarrow \Delta\omega_{N(G)}$ = bandwidth of Gaussian component of modulating noise in PM and FM
12. $\zeta = \tau\,\Delta\omega_N$, correlation variable, cf. (2.43) and (A.6-9) and figures 3.9a through 3.10b; see (A.6-9) for ζ_c
13. $\hat{\tau}' = \hat{\tau} - \beta(\Delta R/c_o)$, with $\hat{\tau} = \tau - \Delta R/c_o$, cf. (2.3a)
14. $\hat{\mu}_F = \mu_F(1+\Gamma')^{1/2}$: normalized FM index; (2.53)
15. $\hat{\mu}_P = \mu_P(1+\Gamma')^{1/2}$: normalized PM index; (2.53)
16. $\hat{\omega} = (\omega-\omega_o)/\Delta\omega_N$ = normalized displaced angular frequency, cf. (2.49)

SPECTRA AND COVARIANCES FOR "CLASSICAL" NONLINEAR SIGNAL PROCESSING PROBLEMS INVOLVING CLASS A NON-GAUSSIAN NOISE

PART I. ANALYTIC RESULTS AND NUMERICAL EXAMPLES

1. INTRODUCTION

Non-Gaussian noise fields play a critical rôle in modern signal processing because of the frequently dominant effects of such noise and interference in a wide variety of applications. Communication theory generally, and specifically telecommunications, electromagnetic and acoustic scattering, man-made and natural ambient noise, optics, and underwater acoustics, are common areas of interest in this respect. In the present report we are concerned primarily with underwater acoustic noise phenomena, but the models and results are canonical, that is, they take forms invariant to the particular physical application in question.

Specifically, we are concerned with various second-order statistics of non-Gaussian noise processes and fields after they have been subjected to different types of nonlinear operations, such as rectification and modulation. A generic problem here is the passage of non-Gaussian noise through a zero-memory nonlinear (ZMNL) device. The desired output statistics are typically the mean (dc), mean intensity (power), the covariance or correlation function, and the associated spectra. These last include wavenumber spectra in the case of noise fields, as well as the more general frequency-wavenumber spectra obtained by joint temporal and spatial Fourier transformations. Typical "classical" problems include: (i) rectification, (ii) determination of output spectra and covariances, (iii) calculation of (output) signal-to-noise ratios, (iv) modulation, (v) demodulation, and (vi) special systems, as for example, the spectrum analyzer. These and other problems involving ZMNL devices are described in detail in [1; chapters 5 and 12 - 17]. What is new here is the

use of the approximate <u>second-order</u> probability density functions and characteristic functions in the above applications when the noise processes are non-Gaussian.

A full treatment is given in a current study by Middleton, [2], which is an expanded version of his recent paper [3], which employs some of the results of the present report, namely, the calculated covariances and spectra. Here, we are content to summarize the pertinent analytic results, the corresponding examples of calculated covariances and spectra, and the various computational procedures associated with their evaluation. The details of the derivations are provided in [2] and [3]. Included here, also, is a selection of illustrations of the analytic results.

2. ANALYTICAL RESULTS: A SUMMARY

In the present study, we address three classical problems where the goals are the calculation of the covariance and associated intensity spectrum. Specifically, we consider:

<u>Problem I</u>. The half-wave ν-th law rectification of Class A noise fields and processes;

<u>Problem II</u>. Phase modulation of a carrier by a Class A noise process; and

<u>Problem III</u>. Frequency modulation of a carrier by a Class A noise process.

Class A noise, as noted in section 3 of [2], [3], is a canonical form of interference characterized by a coherent structure vis-à-vis the (linear) front-end stages of a typical receiver: negligible transients are produced at the output of these stages. Class B noise, on the other hand, is incoherent and highly impulsive, such that the front-end stages of the receiver generate an output which consists solely of (overlapping) transients. Here, the Class A models are tractable in the required second-order distribution and characteristic functions, whereas the Class B models are not and must

consequently be appropriately approximated in second-order; see [4] and [5] for additional information. In the present report, we shall consider examples of Class A noise only.

2.1 THE SECOND-ORDER CLASS A CHARACTERISTIC FUNCTION

In applications [1] - [3], the second-order characteristic function, $F_2(i\xi_1, i\xi_2)$, plays a key rôle: from it, we may obtain the aforementioned statistics of the outputs of ZMNL devices, spectra of angle-modulated carriers, and other usually second-order statistics of various nonlinear operations arising in a variety of communication and measurement operations. (See [2], [3] for further discussion.)

Here, we specifically use the approximate Class A noise characteristic function, F_2, including an additive Gaussian component, given by

$$\boxed{F_2(i\xi_1, i\xi_2)_{A+G} = \exp[-A(2-\rho)] \sum_{m_1,m_2=0}^{\infty} \frac{[A(1-\rho)]^{m_1+m_2}}{m_1!\ m_2!} \times \sum_{n=0}^{\infty} \frac{(A\rho)^n}{n!} \exp\left[-\frac{1}{2} Q^{(2)}_{m_1+n,m_2+n}(\xi_1,\xi_2)\right]} , \qquad (2.1)$$

where A ($=A_A$) is the "overlap" index, and where

$$Q^{(2)}_{m_1+n,m_2+n}(\xi_1,\xi_2) \equiv \xi_1^2\, \sigma^2_{m_1+n} + \xi_2^2\, \sigma^2_{m_2+n} + 2\xi_1\xi_2\, K^{(n)}_{L+G} , \qquad (2.2a)$$

$$\sigma^2_{m+n} \equiv \left(\frac{m+n}{A} + \Gamma'_A\right) \Omega_{2A};\ \Omega_{2A} \equiv \tfrac{1}{2}A\langle B_o^2\rangle = A\langle L^2\rangle;\ \Gamma'_A = \sigma_G^2/\Omega_{2A}; \qquad (2.2b)$$

$$K^{(n)}_{L+G} = \left(n\, k_L/A + k_G\, \Gamma'_A\right) \Omega_{2A}; \qquad (2.2c)$$

and k_L, k_G are the normalized covariances of the non-Gauss and Gauss components, respectively. Thus, $|k_{L,G}| \le 1$.

Here, ρ ($=\rho_A$) is the "overlap" correlation function

$$\rho(\tau') \equiv \begin{Bmatrix} 1-\beta|\tau'| & \text{for } \beta|\tau'| \le 1 \\ 0 & \text{for } \beta|\tau'| > 1 \end{Bmatrix}, \quad \beta = 1/\overline{T}_s , \tag{2.3}$$

in which $\overline{T}_s$ is the mean duration of a typical noise-signal of intensity $\langle B_o^2\rangle/2 = \langle L^2\rangle$. The time delay τ' is given by

$$\tau' = \tau - \frac{\Delta R}{c_o} \quad \text{or} \quad \tau' = \tau \ (= t_2 - t_1) , \tag{2.3a}$$

respectively, for space-time fields and received temporal processes. The path delay $\Delta R/c_o$ ($= |R_2 - R_1|/c_o$) accounts for the time differential between propagation paths to the points at which processing occurs, cf. figure 2.1 ff, Case A. The quantities Ω_{2A} and σ_G^2 are, respectively, the intensity of the non-Gaussian and Gaussian components which constitute the general Class A model used here. (However, we note that the present Class A model belongs either to the strictly canonical Class A cases, where all interfering sources are equidistant from the observer, or more generally, to the much broader class of situations in which the effective source distribution is concentrated in an annulus whose inner-to-outer radii have a ratio O(1/2) or less. The former is exactly represented by (2.1) to second-order, while the latter is approximately so represented, albeit a good approximation as long as the aforementioned source annulus is not too large. See [5; section V, C], for example. For an exact treatment, see also [6], in an important class of physical models. Finally, differentiation of F_2, (2.1), in the usual way, gives us the (exact) covariance of the composite Class A and Gauss field, namely,

$$K_{A+G} = -\frac{\partial^2}{\partial\xi_1\partial\xi_2} F_2 \Big|_{\xi_1=\xi_2=0} = K_A + K_G , \tag{2.4}$$

which in normalized form is

$$k_{A+G}(\Delta R,\tau) = \frac{k_L + \Gamma' \ k_G}{1 + \Gamma'} \ . \tag{2.4a}$$

In practice, A is usually less than unity, say O(0.1 - 0.3) typically, so that only a comparatively few terms in $A^{m_1+m_2+n}$ are needed for numerical evaluation of (2.1) and the statistical quantities derived from it, cf. section 2.2 ff. Note that when $\beta|\tau| \geq 1$, $\rho = 0$, and $\Gamma' = 0$, we get

$$F_{2-A} = \left(e^{-A} \sum_{m=0}^{\infty} \frac{A^m}{m!} \exp\left(-\ \tfrac{1}{2}\xi_1^2\sigma_m^2\right)\right) \left(e^{-A} \sum_{n=0}^{\infty} \frac{A^n}{n!} \exp\left(-\ \tfrac{1}{2}\xi_2^2\sigma_n^2\right)\right)$$

$$= F_1(i\xi_1)_A \ F_1(i\xi_2)_A \ , \tag{2.4b}$$

as expected: there is now no correlation between process samples. With a Gaussian component, these will be correlated, of course, unless $|\tau| \to \infty$, so that $k_G \to 0$, cf. (2.2c).

2.2 PROBLEM I: HALF-WAVE ν-TH LAW RECTIFICATION (STATIONARY AND HOMOGENEOUS FIELDS)

Here we consider the problem of obtaining the second-order (second-moment) statistics, M_y, of a sampled noise field, $\alpha(R,t)$, after passage through a ZMNL device, g, when the noise is generally non-Gaussian. Various processing configurations are possible. We show two in figure 2.1, below. Analytically, we have, for stationary and homogeneous inputs [1; section 2.3-2]

$$M_y(\Delta R,\tau) = \overline{g(x_1)g(x_2)} = \frac{1}{(2\pi)^2} \int_{C_1}\int_{C_2} f(i\xi_1) \ f(i\xi_2)$$

$$\times \ F_2(i\xi_1,i\xi_2;\Delta R,\tau)_x \ d\xi_1 \ d\xi_2 = \overline{y_1 \ y_2} \ , \tag{2.5}$$

where $\Delta R = R_2 - R_1$, $\tau = t_2 - t_1$, and $f(i\xi)$ is the Fourier transform of the ZMNL device with $y_1 = y(R_1,t_1)$, etc. In the present cases, we have specifically

$$f(i\xi) = \beta\, \Gamma(\nu+1)/(i\xi)^{\nu+1} \quad , \quad \nu > -1 \; , \tag{2.6}$$

for these half-wave ν-th law rectifiers [1; (2.101a,b)].

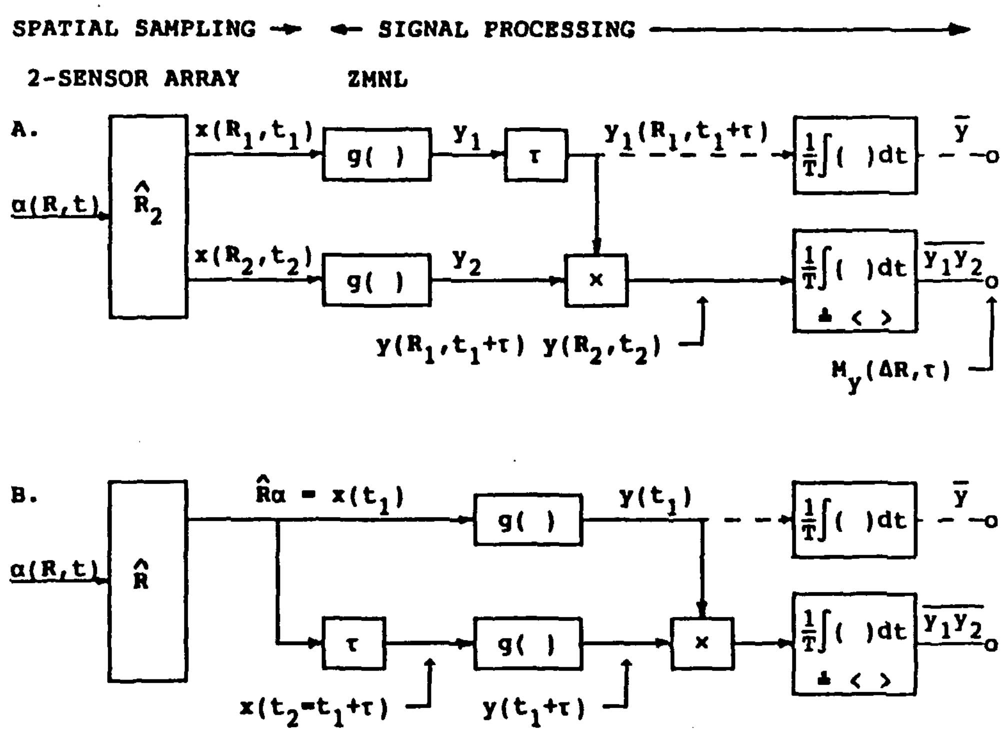

Figure 2.1 A. Two-point sensor array ($\hat{R}_2$) giving sampled field at two space-time points. B. A general array ($\hat{R}$) (preformed beam), converting the field $\alpha(R,t)$ into a single (time) process $x(t_1)$. Both are followed by ZMNL devices, delays, and averaging, as indicated schematically.

For the Class A non-Gaussian noise inputs of section 2.1 above, we find that the (normalized) second-moment M_y for the resulting rectified field is now

$$\boxed{\begin{aligned} M_y(\hat{\Delta R},\tau) &= \exp[-A(2-\rho)] \sum_{m_1,m_2=0}^{\infty} \frac{[A(1-\rho)]^{m_1+m_2}}{m_1!\; m_2!} \sum_{n=0}^{\infty} \frac{(A\rho)^n}{n!} \\ &\quad \times \left(\frac{n+m_1}{A} + \Gamma'\right)^{\nu/2} \left(\frac{n+m_2}{A} + \Gamma'\right)^{\nu/2} B_\nu\Big|_{m_1,m_2,n} \quad , \end{aligned}} \tag{2.7}$$

where we have further postulated the noise field to be isotropic, $\Delta R \to |\Delta R|$, and where specifically,

$$B_\nu\Big|_a \equiv B_\nu(Y|m_1,m_2,n) = \Gamma^2\left(\frac{\nu+1}{2}\right) {}_2F_1\left(-\frac{\nu}{2},-\frac{\nu}{2};\frac{1}{2};Y_a^2\right)$$

$$+ 2Y_a\, \Gamma^2\left(\frac{\nu}{2}+1\right) {}_2F_1\left(\frac{1-\nu}{2},\frac{1-\nu}{2};\frac{3}{2};Y_a^2\right) \quad , \tag{2.7a}$$

$$Y_a \equiv \frac{\frac{n}{A} k_L + \Gamma' k_G}{\left(\frac{m_1+n}{A} + \Gamma'\right)^{\frac{1}{2}} \left(\frac{m_2+n}{A} + \Gamma'\right)^{\frac{1}{2}}} \; ; \quad a = (m_1,m_2,n) \;, \quad |Y_a| \le 1 \;. \tag{2.7b}$$

Specifically, also, we have the following normalized forms

$$\hat{M}_y \equiv M_y/\Omega_{2A}^{\nu} 2^{\nu}/4\pi \; ; \quad \hat{\tau}' \equiv \beta\tau' \;, \quad \beta = 1/\overline{T}_s \;, \quad \text{cf. } (2.3) \;,$$

$$\hat{\Delta R} \equiv \Delta R/\Delta_L \;, \quad \Delta_L = \text{correlation distance}, \quad \Delta R = |R_2-R_1| \;. \tag{2.8}$$

For numerical results, we select the following models for the space-time covariance functions of the isotropic and stationary non-Gaussian and Gaussian components of the input noise field:

$$k_L \equiv \exp\left(-\Delta R^2/\Delta_L^2 - \tfrac{1}{2}(\Delta\omega_L \tau'/\beta)^2\right) = \exp\left(-\hat{\Delta R}^2 - \tfrac{1}{2}(\Delta\hat{\omega}_L \hat{\tau}')^2\right) \; ; \tag{2.9a}$$

$$k_G \equiv \exp\left(-\Delta R^2/\Delta_G^2 - \tfrac{1}{2}(\Delta\omega_G \tau'/\beta)^2\right) = \exp\left(-\hat{\Delta R}^2(\Delta_L/\Delta_G)^2 - \tfrac{1}{2}(\Delta\hat{\omega}_G \hat{\tau}')^2\right) \; ;$$

$$\Delta\hat{\omega}_L \equiv \Delta\omega_L/\beta \ , \quad \Delta\hat{\omega}_G \equiv \Delta\omega_G/\beta \ . \tag{2.9b}$$

Here, Δ_G is a correlation distance, and $\Delta\omega_L$, $\Delta\omega_G$ are angular frequency spreads associated with the respective non-Gaussian and Gaussian components of the input field. Note that if we define the correlation distance Δ_L as that where $k_L = 1/e$ ($\hat{\tau}' = 0$), then $\Delta_L = \Delta R_L$, etc.

For the special cases of ν considered here, we also observe (from [1; (A.1-39)]) that B_ν may be expressed in closed form:

$$B_0(Y) = \pi + 2 \arcsin(Y) \ , \tag{2.10a}$$

$$B_1(Y) = Y \arcsin(Y) + \left(1 - Y^2\right)^{\frac{1}{2}} + \frac{\pi}{2}Y \ , \tag{2.10b}$$

$$B_2(Y) = \left(\frac{1}{2} + Y^2\right)\left(\frac{\pi}{2} + \arcsin(Y)\right) + \frac{3}{2}Y\left(1 - Y^2\right)^{\frac{1}{2}} \ . \tag{2.10c}$$

2.2-1 GAUSS PROCESSES ALONE (A=0)

When only a Gauss noise field is originally present, that is, A = 0, for example, $\Omega_{2A} = 0$, (2.7) reduces to the classical result [1; page 541, (13.4a)]:

$$\boxed{\hat{M}_Y' \equiv \hat{M}_Y\Big|_{A=0} = B_\nu\Big|_{a=0} \ ; \quad M_Y = \frac{(2\psi)^\nu}{4\pi}\hat{M}_Y \ ; \quad Y_a \to Y_o = k_G .} \tag{2.11}$$

For comparison with the non-Gaussian cases (A>0), we choose to have equal <u>input</u> noise intensities. This means that

$$\psi_{A=0} = \sigma_G^2 + \Omega_{2A} = \Omega_{2A}(1 + \Gamma') \ ,$$

so that

$$\hat{M}_Y\Big|_{A=0} = (1 + \Gamma')^\nu \, B_\nu\Big|_{a=0} \ , \quad Y_o = k_G \ , \tag{2.12}$$

and $\hat{M}_Y'$ is then to be compared with $\hat{M}_Y$, $A > 0$. When Γ' is small, as is usually the case, we can often replace $(1 + \Gamma')^\nu$ by unity.

At this point, following figure 2.1, we distinguish two classes of operation: (A), where a pair of point sensors is used to sample the noise field and we wish to consider both the space and temporal correlations of the sampled field at the two points (R_1,t_1), (R_2,t_2); and (B), where the space-time field is converted into a random process, $x(t)$, by the beamforming array $(\hat{R})$, with an associated directionality embodied in the resultant beam (vide [7; sections IV B and VI A]).

2.2-2 CASE B, FIGURE 2.1

Let us consider the simpler case (Case B) of the time process first, cf. (B). For this, we set $\Delta R = 0$ formally in (2.7) et seq. above, since $x = \hat{R}\,\alpha(R,t)$ here and $\tau' = \tau = t_2 - t_1$, cf. (2.3a). See also [3; (3.2) et seq. and (3.11a)]. Then our ad hoc illustrative models of the process covariances k_L, k_G, are, from (2.9a,b), at once*

$$k_L = k_L(\tau) = \exp\left(-\tfrac{1}{2}(\Delta\omega_L\hat{\tau}/\beta)^2\right) = \exp\left(-\tfrac{1}{2}(\Delta\hat{\omega}_L\hat{\tau})^2\right) , \qquad (2.13a)$$

$$k_G = k_G(\tau) = \exp\left(-\tfrac{1}{2}(\Delta\omega_G\hat{\tau}/\beta)^2\right) = \exp\left(-\tfrac{1}{2}(\Delta\hat{\omega}_G\hat{\tau})^2\right) . \qquad (2.13b)$$

Accordingly, (2.7) reduces to

$$\text{Case B:}\quad M_y(0,\hat{\tau}) \equiv M_y(\hat{\tau})_B = (2.7),\ \text{with } Y_a = (2.7b),$$
$$\text{and (2.13a,b) and } \widehat{\Delta R} = 0 \text{ therein.} \qquad (2.14)$$

We note that when $|\hat{\tau}| \geq 1$, $\rho = 0$, and $\hat{M}_y(0,|\hat{\tau}| \geq 1)$ reduces to a simpler relation [vis-à-vis (2.7)], viz.:

---

* A physically derived model of k_G and k_L may be made from [3; (3.11a)] with $L = \hat{R}\,L$, $\hat{R} = (2.9)$ etc., where L is typically given by [3; (3.3)], for example.

$$\boxed{\hat{M}_y(\hat{\tau})_B = e^{-2A} \sum_{m_1,m_2=0}^{\infty} \frac{A^{m_1+m_2}}{m_1!\ m_2!} \left(\frac{m_1}{A} + \Gamma'\right)^{\nu/2} \left(\frac{m_2}{A} + \Gamma'\right)^{\nu/2} B_\nu\Big|_a \,,} \tag{2.14a}$$

where (2.7b) becomes

$$Y_a = \frac{\Gamma' \ k_G}{\left(\frac{m_1}{A} + \Gamma'\right)^{\frac{1}{2}} \left(\frac{m_2}{A} + \Gamma'\right)^{\frac{1}{2}}} \,, \qquad \rho = 0 \,, \tag{2.14b}$$

in $B_\nu\big|_a$.

Special cases of interest are:

I. THE INTENSITY $E(y^2)$: $\hat{\tau} = 0$, $\rho = 1$, $m_1 = m_2 = 0$, and (2.7), (2.14) reduce to

$$\boxed{\overline{y^2}\Big|_{norm} = \hat{M}_y(0)_B = \hat{M}_y(0,0) = B_\nu\Big|_{a=n} = e^{-A} \sum_{n=0}^{\infty} \frac{A^n}{n!} \left(\frac{n}{A} + \Gamma'\right)^{\nu} \,,} \tag{2.15}$$

where now $Y_{a=n} = 1$, e.g., $k_L(0) = 1$ etc., and B_ν is independent of n, for example, for $Y_a = 1$,

$$B_\nu\Big|_{a=n} = \begin{Bmatrix} 2\pi & \text{for } \nu = 0 \\ \pi & \text{for } \nu = 1 \\ 3\pi/2 & \text{for } \nu = 2 \end{Bmatrix} \text{, cf. (2.10) .} \tag{2.16a}$$

For general ν, $Y_a = 1$, we have (from [1; (A.1-34)])

$$B_\nu\Big|_{a=n} = 2\pi^{\frac{1}{2}}\Gamma(\nu+\tfrac{1}{2}) \,, \quad \nu \geq 0 \,. \tag{2.16b}$$

Thus, (2.15) becomes

$$\overline{y^2}\Big|_{norm} = \hat{M}_y(0)_B = \hat{M}_y(0,0) = 2\pi^{\frac{1}{2}}\Gamma(\nu+\tfrac{1}{2})\ e^{-A} \sum_{n=0}^{\infty} \frac{A^n}{n!} \left(\frac{n}{A} + \Gamma'\right)^{\nu} . \tag{2.17}$$

The unnormalized form is, from (2.8),

$$\overline{y^2} = M_y(0)_B = M_y(0,0) = \frac{2^{\nu-1}}{\pi^{1/2}}\,\Omega_{2A}^{\nu}\,\Gamma(\nu+\tfrac{1}{2})\,H_1^{(\nu)}(A,\Gamma') \qquad (2.18)$$

with

$$H_1^{(\nu)}(A,\Gamma') \equiv e^{-A}\sum_{n=0}^{\infty}\frac{A^n}{n!}\left(\frac{n}{A}+\Gamma'\right)^{\nu}$$

$$= \begin{cases} 1 & \text{for } \nu = 0\ , & (2.18a) \\ 1+\Gamma' & \text{for } \nu = 1\ , & (2.18b) \\ 1/A + (1+\Gamma')^2 & \text{for } \nu = 2\ . & (2.18c) \end{cases}$$

For other values of ν (>0), we must evaluate $H_1^{(\nu)}$ numerically.

II. THE MEAN VALUE, $\bar{y}$; $|\hat{t}| \to \infty$

Now $\rho = 0$, $n = 0$, $Y_a = 0$, and (2.7) reduces directly, upon use of (2.18), to

$$\boxed{\begin{aligned} \bar{y}^2\Big|_{norm} &= \hat{M}_y(\infty)_B = \hat{M}_y(0,\infty) = \Gamma^2\left(\frac{\nu+1}{2}\right)\left\{e^{-A}\sum_{m=0}^{\infty}\frac{A^m}{m!}\left(\frac{m}{A}+\Gamma'\right)^{\nu/2}\right\}^2 \\ &= \Gamma^2\left(\frac{\nu+1}{2}\right)H_1^{(\nu/2)}(A,\Gamma')^2\ . \end{aligned}}$$

(2.19)

The unnormalized form of (2.19) is, from (2.8),

$$\bar{y}^2 = M_y(\infty)_B = M_y(0,\infty) = \frac{2^{\nu}\,\Omega_{2A}^{\nu}}{4\pi}\,\Gamma^2\left(\frac{\nu+1}{2}\right)H_1^{(\nu/2)}(A,\Gamma')^2\ , \qquad (2.20)$$

and for ν even, we find, from (2.18a,b,c)

$$H_1^{(0)} = 1\ ,\quad H_1^{(1)} = 1+\Gamma'\ ,\quad H_1^{(2)} = \frac{1}{A} + (1+\Gamma')^2\ . \qquad (2.21)$$

III. THE CONTINUUM INTENSITY: $\overline{y^2} - \bar{y}^2$

From (2.18) and (2.20) we get at once the general result for $\nu \geq 0$,

$$\boxed{P_c \equiv \overline{y^2} - \bar{y}^2 = 2^{\nu}\, \Omega_{2A}^{\nu} \left\{ \frac{\Gamma(\nu+\frac{1}{2})}{2\pi^{\frac{1}{2}}}\, H_1^{(\nu)} - \left[\frac{\Gamma\left(\frac{\nu+1}{2}\right)}{2\pi^{\frac{1}{2}}}\, H_1^{(\nu/2)} \right]^2 \right\},} \quad (2.22)$$

which is the generalization of [1; (13.7)], in the classical purely Gaussian cases, to the present, dominant non-Gaussian noise component Ω_{2A} ($\gg \sigma_G^2$). In these classical cases, we can show at once that

$$\lim_{\Omega_{2A}\to 0} H_1^{(\nu)}\, \Omega_{2A}^{\nu} \to \lim_{\Omega\to 0} e^{-A} \sum_{n=0}^{\infty} \frac{A^n}{n!} \left(\frac{n\Omega}{A} + \sigma_G^2 \right)^{\nu} \to \sigma_G^{2\nu} \; (= \psi^{\nu}) \; , \quad (2.23)$$

where $\Omega_{2A} \to \infty$ implies $A \to 0$ and $\overline{B_0^2} \to 0$, cf. (2.2b), so that (2.22) becomes, as expected,

$$P_c\Big|_{Gauss} = 2^{\nu}\, \sigma_G^{2\nu} \left\{ \frac{\Gamma(\nu+\frac{1}{2})}{2\pi^{\frac{1}{2}}} - \frac{\Gamma^2\left(\frac{\nu+1}{2}\right)}{4\pi} \right\} \quad (> 0) \; , \quad \nu \geq 0 \; . \quad (2.24)$$

Figure 13.5 of [1] shows (2.24) as a function of rectifier law (ν), as well as (2.18), (2.20) in these Gaussian cases. In the present, more general, situation of Class A noise, the results are more complex, as expected, with now <u>two</u> additional parameters (A,Γ'), descriptive of this much broader class of interference.

2.2-3: CASE A, FIGURE 2.1

We turn now to the more general problem of the covariance of the Class A non-Gaussian random field, sampled according to procedure (A), shown schematically in figure 2.1 earlier. Here, $x = \alpha(R,t)$, sensed at (R_1,t_1), (R_2,t_2), where L = L, cf. (3.3) in [3; (3.2)]. Equation (2.7) applies here, with $\Delta R \neq 0$ (as well as for $\Delta R = 0$), and we use (2.9a,b) for our illustrative examples, which are discussed in section 3 following. At this point, we recall from (2.3a) that the proper time delay to use is $\tau' = \tau - \Delta R/c_o$ in $\rho = \rho(\tau')$, and in some of the structural elements of the noise field covariances, cf. [3; (3.11b,c)].

CASE I: $\hat{\tau}' = 0$

From (2.7), we have $\rho = 1$, $m_1 = m_2 = 1$, giving

$$\hat{M}_y(\hat{\Delta R},0) = e^{-A} \sum_{n=0}^{\infty} \frac{A^n}{n!} \left(\frac{n}{A} + \Gamma'\right)^{\nu} B_\nu \Big|_{a=n} , \quad \rho = 1 , \therefore \tau = \frac{\Delta R}{c_o} , \quad (2.25)$$

where (2.7b) is specifically

$$Y_{a=n} = \frac{\frac{n}{A} k_L(\hat{\Delta R},0) + \Gamma' k_G(\hat{\Delta R},0)}{\frac{n}{A} + \Gamma'} . \quad (2.25a)$$

For calculations, (2.9a,b) are used, with B_ν given by (2.7a), where (2.25a) provides Y_a. When $\hat{\Delta R} = 0$, (2.25) reduces to (2.15) et seq. for the total intensity of the field observed at $R_1 = R_2$.

CASE II: $\hat{\Delta R} \to \infty$, $|\tau'| > 1$

When $\hat{\Delta R} \to \infty$, we obtain different results, depending on τ'. Here $\rho = 0$, $Y_a \to 0$, cf. (2.9a,b) in (2.7b), and therefore $n = 0$. Accordingly, (2.7) becomes

$$\hat{M}_y(\infty, |\tau'| > 1) = \hat{M}_y(\infty,\infty) = \hat{M}_y(0,\infty) = \bar{y}^2_{norm}\ ,\ (2.19)\ . \qquad (2.26)$$

The fact that $\hat{\Delta R} \to \infty$ ensures that $Y_a \to 0$, a behavior similar to that for Case (B) above, when we consider the purely Gaussian noise process, section 2.2-1.

CASE III: $\hat{\Delta R} \to \infty$, $0 < |\tau'| < 1$

Here, $\rho > 0$ while $Y_a \to 0$, so that B_ν, (2.7b), becomes $\Gamma^2(\nu+\frac{1}{2})$ once more. The second moment function (2.7) is now

$$\boxed{\begin{aligned} M_y(\hat{\Delta R},\tau') = \Gamma^2\left(\frac{\nu+1}{2}\right) \exp[-A(2-\rho)] \sum_{m_1,m_2=0}^{\infty} \frac{[A(1-\rho)]^{m_1+m_2}}{m_1!\ m_2!} \\ \times \sum_{n=0}^{\infty} \frac{(A\rho)^n}{n!} \left(\frac{n+m_1}{A} + \Gamma'\right)^{\nu/2} \left(\frac{n+m_2}{A} + \Gamma'\right)^{\nu/2}, \end{aligned}} \qquad (2.27)$$

which is a minor simplification of (2.7).

CASE IV: $\hat{\Delta R} \to \infty$, $|\tau'| = 0$

In this special situation, where $\tau = \Delta R/c_o \to \infty$ in such a way that $\tau' = 0$ and therefore $\rho = 1$, $Y_a = 0$, we obtain directly from (2.27) the comparatively simple result,

$$\boxed{\hat{M}_y(\infty,0) = \Gamma^2\left(\frac{\nu+1}{2}\right) H_1^{(\nu)} \quad (> 0)\ .} \qquad (2.28)$$

2.2-4: REMARKS

At first glance, as $\Delta R \to \infty$, we might expect M_y always to reduce to $\bar{y}^2$, e.g., $K_y \equiv M_y - \bar{y}^2 = 0$ for the covariance of the rectified space-time field. This is expectedly the case for the covariance (and second-moment) function of the input Class A and Gauss noise field components $\alpha(R,t)$, as we can see directly from (2.9a,b), or from [3; (3.11b,c)] for example, in the physically derived cases. However, the process or field $y = g(x)$ here is the result of a nonlinear operation, cf. (2.5), (2.6), which severely distorts the input waveform and generates all kinds of modulation products, associated with the spatial as well as the temporal variations of the input field. This accounts for the departures in Cases III, IV of $M_y(\infty,\hat{\tau}')$ from $\bar{y}^2$, while certainly $M_x(\infty,\tau') \to \bar{x}^2 = 0$, (since $\bar{x} = 0$ initially here).

From the various limiting results above, we see that

$$M_y(0,0) > M_y(\infty,0) \quad \text{and} \quad M_y(0,0) > M_y(0,\infty) \ , \tag{2.29a}$$

and

$$M_y(\infty,0) \gtreqless M_y(0,\infty) \quad \text{depending on } A,\ \Gamma', \text{ and } \nu \ , \tag{2.29b}$$

with

$$M_y(0,0) - M_y(0,\infty) > 0 \ , \quad \text{cf. (2.19) and (2,20)} \ , \tag{2.29c}$$

$$M_y(\infty,\infty) = M_y(0,\infty) = \bar{y}^2 \ , \text{ cf. (2.20) and (2.26)} \ , \tag{2.29d}$$

whereas

$$M_x(0,0) > M_x(0,\infty) = M_x(\infty,0) = \bar{x}^2 = 0 \ . \tag{2.29e}$$

Finally, we note that (2.11), (2.12) apply here, also, for the Gauss-alone cases, where now

$$\Omega_{2A}(1 + \Gamma') \to \sigma_G^2 \quad \text{and} \quad B_\nu\Big|_{a=0} \to (1 + \Gamma')^\nu\, B_\nu\Big|_a = 0 \ .$$

2.2-5: SPECTRA

The various intensity spectra associated with the output of the processor (cf. figure 2.1) are important also, as they show how the energy in this output is distributed. Here, we consider two types of spectra, respectively, for the rectified spatial field (A) and for the process (B), namely the wavenumber and the frequency spectrum of $y(R,0)$ and $y(0,t)$. In particular, wavenumber spectra are useful in the analysis of spatially distributed phenomena, paralleling the analysis of time-dependent phenomena.

I: WAVENUMBER SPECTRUM

The wavenumber intensity spectrum is defined here by

$$W_2(k,0)_y = W_2(k,\tau)_y\Big|_{\tau=0} \equiv \iint_{\Delta R} M_y(\Delta R,0)\ \exp(i\mathbf{k}\cdot\Delta\mathbf{R})\ d(\Delta R) \tag{2.30a}$$

$$= 2\pi \int_0^\infty M_y(\Delta R,0)\ J_o(k\Delta R)\ \Delta R\ d(\Delta R) = W_2(k,0)_y\ , \tag{2.30b}$$

with

$$\mathbf{k} = (k_x,k_y)\ ,\quad \Delta R = |\Delta\mathbf{R}|\ ,\quad k = |\mathbf{k}| \tag{2.30c}$$

for these <u>isotropic</u> <u>fields</u>, where $\mathbf{k}$ is an (angular) vector wavenumber. Using the normalization of (2.8), we get, with $\hat{k} \equiv k\Delta_L$,

$$\boxed{\hat{W}_2(\hat{k},0)_y \equiv \frac{W_2(k,0)_y}{\Delta_L^2\ 2^\nu\ \Omega^{2\nu}/4\pi} = 2\pi \int_0^\infty \hat{M}_y(x,0)\ J_o(\hat{k}x)\ x\ dx} \tag{2.31}$$

for the normalized wavenumber intensity spectrum.

Since $\hat{M}_y(\infty,0)$ is nonvanishing, cf. (2.28), there is a dc component, or δ-function, in the general wavenumber spectrum. We will use the relations

$$\int_0^\infty x\, J_o(\hat{k}x)\, dx = \frac{1}{\hat{k}}\,\delta(\hat{k} - 0)\ ,\quad \hat{k} = \left(\hat{k}_x^2 + \hat{k}_y^2\right)^{1/2} = |\hat{\mathbf{k}}|\ ,\quad \hat{\mathbf{k}} = (\hat{k},\phi)\ , \tag{2.32}$$

where we must remember that $\hat{\mathbf{k}}$ is two-dimensional. With ν a vector wavenumber defined by

$$\hat{\mathbf{k}} = 2\pi\hat{\boldsymbol{\nu}}\ [= (\hat{\nu},\phi)]\ ,\quad \hat{k} = 2\pi\hat{\nu} = 2\pi|\hat{\boldsymbol{\nu}}|\ , \tag{2.33a}$$

and using the relation

$$\delta(ax - b) = \frac{1}{a}\,\delta\left(x - \frac{b}{a}\right)\quad \text{for } a > 0\ , \tag{2.33b}$$

we also show that

$$\delta(\hat{k}_x-0)\ \delta(\hat{k}_y-0) = \frac{1}{2\pi\hat{k}}\,\delta(\hat{k}-0) = \frac{1}{(2\pi)^3\hat{\nu}}\,\delta(\hat{\nu}-0)$$

$$= \frac{1}{(2\pi)^2}\,\delta(\hat{\nu}_x-0)\ \delta(\hat{\nu}_y-0)\ ,\quad \hat{\nu} = |\hat{\boldsymbol{\nu}}|\ ,\quad \hat{\nu} = \left(\hat{\nu}_x^2 + \hat{\nu}_y^2\right)^{1/2}\ . \tag{2.34}$$

Applying (2.32) - (2.34), with

$$\hat{W}_2(\hat{k},\phi)_y = 2\pi\int_0^\infty x\, J_o(\hat{k}x)\left[\hat{M}_y(x,0) - \hat{M}_y(\infty,0)\right] dx$$

$$+ 2\pi\,\hat{M}_y(\infty,0)\int_0^\infty x\, J_o(\hat{k}x)\, dx \tag{2.35a}$$

$$\boxed{\begin{aligned} &= \hat{W}_2(\hat{k},0)_{y\text{-cont}} + (2\pi)^2\,\hat{M}_y(\infty,0)\ \delta(\hat{k}_x-0)\ \delta(\hat{k}_y-0) \\ &= \hat{W}_2(\hat{k},0)_{y\text{-cont}} + \hat{M}_y(\infty,0)\ \delta(\hat{\nu}_x-0)\ \delta(\hat{\nu}_y-0)\ , \end{aligned}} \tag{2.35b}$$

which defines $\hat{W}_2(\hat{k},0)_{y\text{-cont}}$, the continuous portion of the spectrum and shows the dc term in $\hat{k}$- or $\hat{\nu}$-space, as convenient. It is $\hat{W}_{2\text{-cont}}$ with which we are concerned in the specific numerical examples of section 3 ff.

II. FREQUENCY SPECTRUM

Here we employ the Wiener-Khintchine theorem [1; (3.42)] to write for the frequency spectrum of y

$$W_y(f) = 2\int_{-\infty}^{\infty} M_y(0,\tau)\,\exp(-i\omega\tau)\,d\tau = B_o\int_0^{\infty}\hat{M}_y(0,\hat{\tau})\,\cos(\hat{\omega}\hat{\tau})\,d\hat{\tau}\,, \tag{2.36}$$

where

$$B_o \equiv \Omega_{2A}^{\nu}\,2^{\nu}/\pi\beta;\quad \hat{\tau} = \beta\tau;\quad \omega = 2\pi f;\quad \hat{\omega} \equiv \omega/\beta;\ \therefore\ \hat{f} = f/\beta. \tag{2.36a}$$

Accordingly, we define the normalized frequency intensity spectrum of y as

$$\boxed{\hat{W}_y(\hat{f}) \equiv W_y(f)/B_o = \int_0^{\infty}\hat{M}_y(0,\hat{\tau})\,\cos(\hat{\omega}\hat{\tau})\,d\hat{\tau}\ .} \tag{2.37}$$

Again, there is a dc component, since $\hat{M}_y(0,\infty) = \bar{y}^2$ (> 0), cf. (2.20). We have

$$\hat{W}_y(f) = \int_0^{\infty}\left[\hat{M}_y(0,\hat{\tau})-\hat{M}_y(0,\infty)\right]\cos(\hat{\omega}\hat{\tau})\,d\hat{\tau} + \frac{1}{2}\,\hat{M}_y(0,\infty)\,\delta(\hat{f}-0), \tag{2.38}$$

since

$$\int_0^{\infty}\cos(\omega x)\,dx = \pi\,\delta(\omega-0) = \frac{1}{2}\,\delta(f-0)\ .$$

As in the wavenumber cases above (Case I), we are concerned with the continuous part of the spectrum, viz.

$$\boxed{\hat{W}_y(f)_{cont} = \int_0^{\infty} \left[\hat{M}_y(0,\hat{\tau}) - \bar{y}^2\right] \cos(\omega\hat{\tau})\, d\hat{\tau}\ ,} \qquad (2.39)$$

which is also illustrated numerically in section 3 ff.

III. WAVENUMBER FREQUENCY SPECTRUM

The wavenumber frequency spectrum is defined by

$$W_2(k,\omega)_y = \iint_{-\infty}^{\infty} M_y(\Delta R,\tau)\, \exp(ik\cdot\Delta R - i\omega\tau)\, d(\Delta R)\, d\tau\ , \qquad (2.40)$$

with $\omega = 2\pi f$. The associated wavenumber spectrum $W_2(k,0)$ used in (2.30) is obtained from $W_2(k,\tau)\big|_{\tau=0}$. In normalized form, we have for (2.40), in these isotropic cases,

$$\hat{W}_2(\hat{k},\hat{\omega})_y = \left(2^{\nu}\, \Omega_{2A}^{\nu}\, \Delta_L^2/(4\pi\beta)\right)^{-1} W_2(k,\omega)_y$$

$$= \iint_{-\infty}^{\infty} \hat{M}_y(\hat{\Delta R},\hat{\tau})\, \exp(i\hat{k}\cdot\hat{\Delta R} - i\hat{\omega}\hat{\tau})\, d(\hat{\Delta R})\, d\hat{\tau}\ ;$$

$$\boxed{\hat{W}_2(\hat{k},\hat{\omega})_y = 2\pi \int_0^{\infty}\int_0^{\infty} \hat{M}_y(x,\hat{\tau})\, J_o(\hat{k}x)\, \exp(-i\hat{\omega}\hat{\tau})\, x\, dx\, d\hat{\tau}\ .} \qquad (2.41)$$

The various dc components are readily extracted, as in Cases I and II above. Numerical examples of this joint intensity spectrum are reserved to a possible subsequent study. The results of section 3 show the marginal spectra (Cases I, II) of this more general situation.

2.2-6: FREQUENCY AND PHASE MODULATION BY CLASS A AND GAUSSIAN NOISE

This is a Case (B) situation, cf. figure 2.1, where $\Delta R = 0$ and we are concerned only with the received (non-Gaussian) noise process which is used to angle-modulate a (high frequency) carrier f_o. For the analysis, see [3; section II].

The general result for the covariance of the carrier modulated by Class A and Gauss noise is found to be

$$\boxed{K_y(\tau)_{A+G} = \tfrac{1}{2}A_o^2 \,\mathrm{Re}\left[\exp\left(i\omega_o\tau - D_o^2\Omega(\tau)_G - A(2-\rho) + 2A(1-\rho)\exp\left[-D_o^2\Omega_o/A\right]\right)\right]} \,, \tag{2.42}$$

where now, cf. [1; (4.2),(14.14c)],

$$\Omega(\tau)_{\substack{G\\A}}\Big|_{FM} = \left(\sigma_G^2 \text{ or } \tfrac{1}{A}\Omega_{2A}\right)\int_0^{|\tau|}(|\tau|-\lambda)\,k(\lambda)\,d\lambda \qquad (D_o = D_F)$$

$$= \left(1 \text{ or } \tfrac{1}{A}\right)\int_0^{\infty} W_{(G \text{ or } L)}(f)\,\frac{1-\cos(\omega\tau)}{\omega^2}\,df \,. \tag{2.42a}$$

Also, cf. [1; (14.2), (14.14c)],

$$\Omega(\tau)_{\substack{G\\A}}\Big|_{PM} = \left(\sigma_G^2 \text{ or } \tfrac{1}{A}\Omega_{2A}\right)\{k(0) - k(\tau)\}_{(G \text{ or } L)} \qquad (D_o = D_P) \tag{2.42b}$$

and

$$\Omega_o \to \Omega_o\Big|_{FM} = \int_0^{\infty} W_A(f)\,df/\omega^2 \quad \text{or} \quad \Omega_o\Big|_{PM} = \Omega_{2A} \,. \tag{2.42c}$$

For our numerical examples, we use the RC-spectrum of [1; section 14.1-3], where now

$$k_L(\zeta) = \exp(-b|\zeta|) \ , \quad k_G(\zeta) = \exp(-|\zeta|) \ , \quad \zeta = \tau \ \Delta\omega_N \ , \qquad (2.43)$$

and therefore

$$\text{FM:} \quad D_F^2 \ \Omega(\tau)_A = \frac{1}{Ab^2} \left(\mu_F^2\right)_A [\exp(-b|\zeta|) + b|\zeta| - 1] \ ;$$

$$D_F^2 \ \Omega(\tau)_G = \Gamma' \left(\mu_F^2\right)_A [\exp(-|\zeta|) + |\zeta| - 1] \ ;$$

$$\left(\mu_F^2\right)_A = \Omega_{2A} \ D_F^2/\Delta\omega_N^2 \ ; \qquad (2.44a)$$

$$\text{PM:} \quad D_P^2 \ \Omega(\tau)_A = \frac{1}{A}\left(\mu_P^2\right)_A [1 - \exp(-b|\zeta|)] \ ;$$

$$D_P^2 \ \Omega(\tau)_G = \Gamma' \left(\mu_P^2\right)_A [1 - \exp(-b|\zeta|)] \ ;$$

$$\left(\mu_P^2\right)_A = D_P^2 \ \Omega_{2A} \ , \qquad (2.44b)$$

with b (> 0) a dimensionless quantity, as is ζ. The quantity $\Delta\omega_N$ is the bandwidth of the modulating (Gauss) noise, cf. (2.43). Note, also, that

$$\Gamma' \left(\mu_F^2\right)_A = \sigma_G^2 \ D_F^2/\Delta\omega_N^2 = \left(\mu_F^2\right)_G \ ; \quad \Gamma' \left(\mu_P^2\right)_A = \sigma_G^2 \ D_P^2 = \left(\mu_P^2\right)_G \ . \qquad (2.45)$$

The quantities $(\mu_{F,P}^2)_{()}$ are the respective modulation indexes for FM and PM, cf. [1; chapter 14].

Finally, we have for ρ in (2.3), now with $\Delta R = 0$,

$$\rho(\tau) \rightarrow \rho(\zeta) = \begin{Bmatrix} 1 - \dfrac{\beta|\zeta|}{\Delta\omega_N} & \text{for} \ \dfrac{\beta|\zeta|}{\Delta\omega_N} \le 1 \\ 0 & \text{for} \ \dfrac{\beta|\zeta|}{\Delta\omega_N} > 1 \end{Bmatrix} . \qquad (2.46)$$

Putting the above (2.43), (2.44) in (2.42), we now specialize our results,

$$K_y(\tau)_{A+G} = \tfrac{1}{2}A_o^2\, k_o(\tau)\cos(\omega_o\tau)\ , \quad \text{with} \quad k_o(0) = 1\ , \qquad (2.47)$$

to the normalized covariance $k_o(\tau)$, respectively, for FM and PM, and their associated spectra. We have for these carriers modulated by a sum of Gaussian and Class A noise:

I. FREQUENCY MODULATION

$$\boxed{\begin{aligned} k_o(\zeta)_{FM} = \exp\Big[-\Gamma'\left(\mu_F^2\right)_A [\exp(-|\zeta|) + |\zeta| - 1] - A(2-\rho) \\ + A\rho\exp\left(-\frac{1}{Ab^2}\left(\mu_F^2\right)_A [\exp(-b|\zeta|) + b|\zeta| - 1]\right)\Big]\ , \end{aligned}} \qquad (2.48)$$

with $\rho(\tau)$ given by (2.46). Here, $\Omega_o\big|_{FM} \to \infty$ in (2.42). Since

$$\lim_{\zeta\to\infty} k_o(\zeta)_{FM} = 0\ ,$$

there is no dc in k_{o-FM}, and hence all the original carrier power $(\sim A_o^2/2)$ is distributed into the sideband continuum for this highly nonlinear modulation, as expected [1; section 14.1-2].

The associated intensity spectrum for $k_o\big|_{FM}$ is defined by

$$W(\hat{\omega})_{A+G}\Big|_{FM} = \int_0^\infty k_o(\zeta)_{FM}\cos(\hat{\omega}\zeta)\, d\zeta\ , \quad \hat{\omega} \equiv \frac{\omega-\omega_o}{\Delta\omega_N}\ , \qquad (2.49)$$

which is determined by a direct cosine transform of $k_o(\zeta)_{FM}$. See appendix A.6 ff.

II. PHASE MODULATION

$$\boxed{\begin{aligned} k_o(\zeta)_{PM} = \exp\Big[&-\Gamma'\left(\mu_P^2\right)_A [1 - \exp(-|\zeta|)] + 2A(1-\rho)\exp\left(-\tfrac{1}{A}\left(\mu_P^2\right)_A\right) \\ &- A(2-\rho) + A\rho\exp\left(-\tfrac{1}{A}\left(\mu_P^2\right)_A [1 - \exp(-b|\zeta|)]\right)\Big] \;, \end{aligned}} \tag{2.50}$$

with $\rho(\zeta)$ again given by (2.46). We note that

$$k_o(0)_{PM} = 1 \;, \tag{2.51a}$$

as before; that is, the total (normalized) intensity is unity. Also

$$\boxed{k_o(\infty)_{PM} = \exp\left[-\Gamma'\left(\mu_P^2\right)_A - 2A\left(1 - \exp\left(-\tfrac{1}{A}\left(\mu_P^2\right)_A\right)\right)\right] \;:} \tag{2.51b}$$

this is the fraction of the power remaining in the carrier, so that

$$k_o(0)_{PM} - k_o(\infty)_{PM} = 1 - (2.51b) \;, \tag{2.51c}$$

which is the fraction of the power distributed in the sideband continuum.

The associated intensity spectrum of the sideband continuum is determined from

$$w(\hat{\omega})_{A+G}\Big|_{PM\text{-}cont} = \int_0^\infty \left[k_o(\zeta)_{PM} - k_o(\infty)_{PM}\right] \cos(\hat{\omega}\zeta)\, d\zeta \;. \tag{2.52}$$

See section 3 ff. for examples and appendix A.5 for the evaluation methods.

Finally, in the equivalent Gaussian cases (Gauss noise modulation of equal intensity and basic spectrum, e.g.,

$$\Gamma' \left(\mu_F^2\right)_A \rightarrow \Gamma' \left(\hat{\mu}_F^2\right)_A = \Gamma' \mu_{FA}^2 (1 + \Gamma') \quad \text{and} \quad k_G \rightarrow k_L ,$$

we see that (2.48), (2.50) reduce to

$$k_o(\zeta)_{FM\text{-}Gauss} = \exp\left[-\left(\hat{\mu}_F^2\right)_A \Gamma' \left[\exp(-b|\zeta|) + b|\zeta| - 1\right]/b^2\right] ,$$

$$\left(\hat{\mu}_F^2\right)_A = (1 + \Gamma')\left(\mu_F^2\right)_A ; \qquad (2.53a)$$

$$k_o(\zeta)_{PM\text{-}Gauss} = \exp\left[-\left(\hat{\mu}_P^2\right)_A \Gamma' \left[1 - \exp(-b|\zeta|)\right]\right] ,$$

$$\left(\hat{\mu}_P^2\right)_A = (1 + \Gamma')\left(\mu_P^2\right)_A , \qquad (2.53b)$$

with spectra obtained as before, from (2.49) and (2.52).

3. NUMERICAL ILLUSTRATIONS AND DISCUSSION

It is convenient to discuss the general results, namely the effects of (ZMNL) nonlinear rectifiers on, and modulation by, a mixture of Gaussian and non-Gaussian noise processes and fields, from the specific numerical calculations presented here in figures 3.1 - 3.10. These constitute a representative selection from the universe of possible parameter states [cf. "Summary of Normalized Parameters" and section 2, preceding]. This is done here on a per-figure basis, as noted below. In each case, the dc component is removed: only the covariance or continuous spectrum is calculated. We recall that there are two cases to distinguish: Case A, $\tau'=\tau-\Delta R/c_0$, a 2-element array; and Case B, $\tau'=\tau=t_2-t_1$, a preformed beam. See figure 2.1 and (2.3a).

All spectra shown here are normalized to have area (under the spectrum level) of unity, i.e., the spectral normalization is obtained by dividing the spectrum by the value of the associated covariance at its origin. The normalization of the covariances themselves is obtained by dividing by the value at $\hat{\tau}=0$ or $\hat{\Delta R}=0$.

I. GAUSS NOISE ALONE

FIGURE 3.1

This figure shows the normalized <u>temporal</u> <u>covariance</u> ($\hat{\Delta R}=0$) for both the input and output of a ZMNL half-wave ν-th law ($\nu\geq 0$) detector, when $\nu = 0,1,2$ and when only Gaussian noise (A=0) is applied to these nonlinear devices. These curves are based on (2.11) with (2.7a), where $Y_a = k_G$, (2.96), with $\Delta\hat{\omega}_G \equiv \Delta\omega_G/\beta = 5$ here. The normalization is with respect to the covariance maximum; e.g., the normalized covariance shown in figure 3.1 is obtained from $[(2.11)/(2.11)_{\hat{\tau}=0}]$, $\hat{\Delta R}=0$. These results apply for both cases A,B of figure 2.1, where now $\hat{\tau}'=\hat{\tau}$, since $\hat{\Delta R}=0$, cf. (2.3a) and remarks.

As expected (cf. [1; chapter 13]), the general nonlinearity (2.6), $\nu \geq 0$, contracts the covariance, which is equivalent to spreading the spectrum vis-à-vis the input , cf. figure 3.2, below. Moreover, the greater the distortion (ν=0,2), usually the greater are these effects. [See appendix A.1.]

FIGURE 3.2

This is the same situation as shown in figure 3.1, except that the normalized intensity (frequency) spectrum is calculated now [cf. section 2.2-5, Case II, (2.39)] with $\hat{M}_y(0,\hat{\tau})$, (2.11), used in (2.39). Observe the greatly broadened spectra, particularly at the low spectral levels, where the greater spread occurs for the "super-clipper", ν=0, cf. remarks, figure 3.1; also, appendix A.3.

FIGURE 3.3

For the same purely Gaussian field above, cf. (2.11) and (2.96), with $\hat{\tau},\hat{\tau}'=0$, the spatial covariance is calculated, with parameters $\Delta_L/\Delta_G = 5^{\frac{1}{2}}$, using (2.11) as before. The normalization is with respect to the covariance at $\widehat{\Delta R}=0$. Again, one observes the same kind of contraction in the covariance as noted in figure 3.1. [See appendix A.2.]

FIGURE 3.4

This is the wavenumber analogue of the frequency spectrum of figure 3.2, now with $\hat{\tau}',\hat{\tau}=0$, and is obtained from (2.35a,b) with $\Delta_L/\Delta_G = 5^{\frac{1}{2}}$. The rectification operation similarly spreads the wavenumber spectrum, with the greatest distortion (ν=0) yielding the greatest wavenumber spread, as expected from the corresponding contraction of the associated covariance, cf. figure 3.3 above. [See appendix A.4.]

CLASS A PLUS GAUSS NOISE

FIGURE 3.5

The temporal covariance here is given by the general result (2.7), with the associated relations (2.7), (2.8), (2.9), wherein $\Delta\hat{R}=0$, so that $\hat{\tau}=\hat{\tau}'=t_2-t_1$, as before, and where $B_\nu|_a$, (2.7a), is now given analytically by (2.10) for $\nu = 0,1,2$. Here, the parameter values are $\Delta\hat{\omega}_G \equiv \Delta\omega_G/\beta = 5^{1/2}$, as before, now with $A=0.2$, $\Gamma_A'=10^{-3}$, $\Delta\omega L/\beta \equiv \Delta\hat{\omega}_L = 1$ for the Class A non-Gaussian noise component, typically.

Again, for the super-clipper ($\nu=0$), the contraction in the normalized covariance is greatest, cf. figure 3.1. But the contribution of the comparatively strong non-Gaussian component exaggerates this effect. [See appendix A.1.]

FIGURE 3.6

The corresponding intensity (frequency) spectrum ($\Delta\hat{R}=0$), obtained from (2.7) in (2.39), however, shows a fine-structure not exhibited when Gauss noise alone ($A=0$) is applied to these ZMNL devices. The spectral levels for the case $\nu=0$, ($A=0$) and ($A>0$), cf. figure 3.2 with figure 3.6, are approximately the same, whereas the other inputs, cases $\nu=1,2$, are much elevated as f becomes larger, again due to the presence of the structured Class A noise, when $\beta\bar{T}_S \leq 1$, cf. (2.3): on the average, the original Class A "signals" are of comparatively short duration, or spectrally wide to begin with, so that clipping further spreads the spectrum. [See appendix A.3.]

FIGURE 3.7

The spatial covariance when Class A noise is added to the Gaussian input shows analogous behavior, cf. figures 3.3 and 3.5: the covariance is compressed vis-à-vis the input, but more so than in the Gauss-alone situations. Again, (2.7) - (2.10) are employed. [See appendix A.2.]

FIGURE 3.8

The corresponding wavenumber (intensity) spectrum with Class A noise and the Gaussian component, obtained from (2.7) - (2.10) in (2.39), is shown here. Comparison with figure 3.4 indicates a broader spectral input, due to the non-Gaussian component, but a relatively narrower output, although the latter is still noticeably spread vis-à-vis the original input. [See appendix A.4.]

FIGURE 3.9

Finally, we consider the angle-modulation cases described in section 2.2-6 above, where weak to strong angle modulations ($\mu \sim 1$ to 50) by Class A noise, with a weak ($\Gamma' = 10^{-3}$) Gaussian modulation component, is employed.

For phase modulation by non-Gaussian noise, based on (2.50) with (2.44b), (2.45), (2.46), the resulting normalized intensity (frequency) spectra are obtained by applying (2.50) to (2.52), where $f = \hat{\omega}/2\pi$; $\hat{\omega} = (\omega - \omega_0)/\Delta\omega_N$, cf. (2.49). Note the "spike" at $f \sim 0.1$, followed by a variety of sidelobes which rise as the phase modulation index μ_P increases. The spike is now bounded at $f \simeq 0.8$, at the -10 dB level, when $\mu_P = 50$. As expected, the larger indexes (μ_P) produce broader spectra. [See appendix A.5.]

FIGURE 3.10

For frequency modulation by non-Gaussian noise, from (2.48) with (2.49) and (2.44a), the corresponding intensity (frequency) spectra again exhibit a continuous spike ($f < 0.1$). With small modulation indexes (μ_F), the spectra are less broad than for the larger indexes, as expected. The non-Gaussian noise component dominates the spectrum here. [See appendix A.6.]

EXTENSIONS

Other situations where the second-order Class A probability density functions may be applied are noted in [2] and [3]. We list some of the extensions of the analysis to the following "classical" problems:

1) The inclusion of representative signals, with Gauss and non-Gauss (Class A) noise, in the problems already treated here (section 2);
2) The case of the full-wave square-law rectifier, with both Class A and B noise, as well as Gauss noise;
3) The extension of 2) to include general broadband and narrowband signals;
4) The calculation of signal-to-noise ratios and deflection criteria, cf. [1; section 5.3-4].
5) Covariances and spectra for ZMNL system outputs, with signals as well as non-Gaussian noise inputs;
6) The rôle of the electromagnetic (or acoustic) interference (EMI or AcI) scenario, cf. [5; section 2B,5];
7) Evaluation of the large (FM,PM) indexes, or asymptotically Gaussian cases, cf. [12].

Further opportunities to extend the classical theory [2],[3], now with non-Gaussian noise inputs, are evident from the examples and methods described in [1; chapters 5, 12 - 16], for instance.

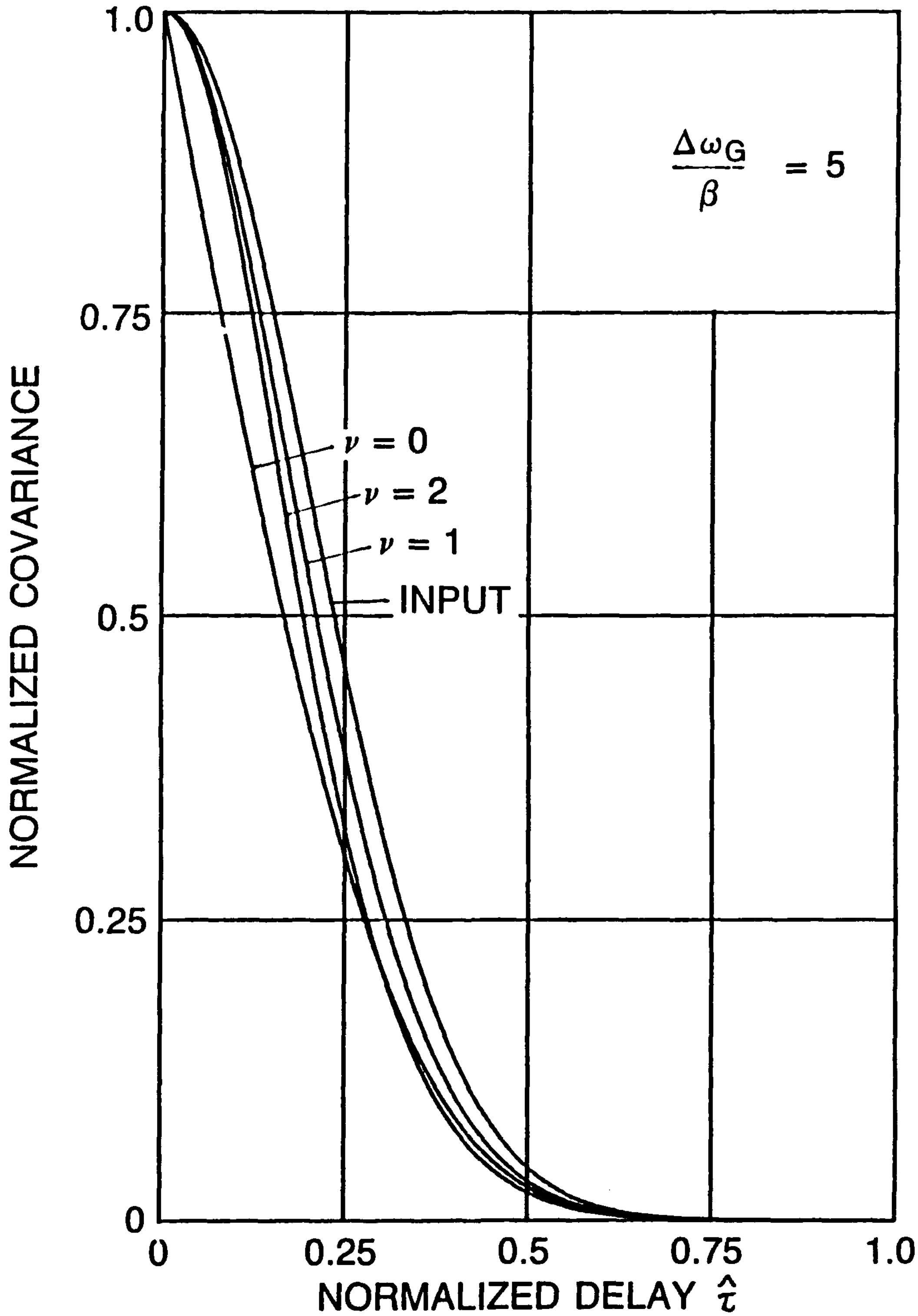

FIGURE 3.1 TEMPORAL COVARIANCE (FOR $\widehat{\Delta R}=0$); GAUSS NOISE ONLY; CF. (2.11) WITH (2.7a), (2.9b), AND APPENDIX A.1

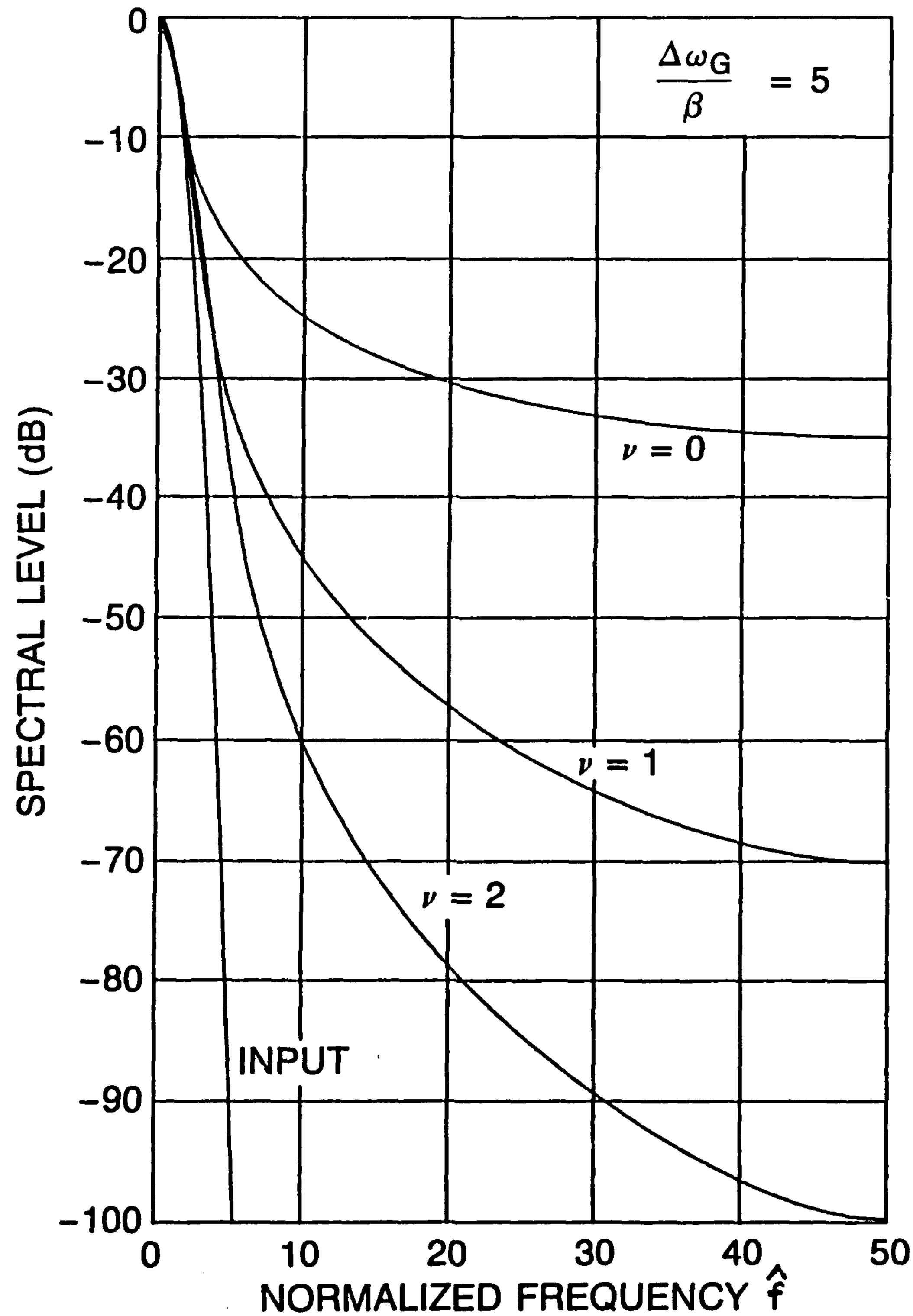

FIGURE 3.2 FREQUENCY (INTENSITY) SPECTRUM (FOR $\hat{\Delta R}=0$); GAUSS NOISE ONLY; CF. (2.39), USED WITH (2.11), AND APPENDIX A.3

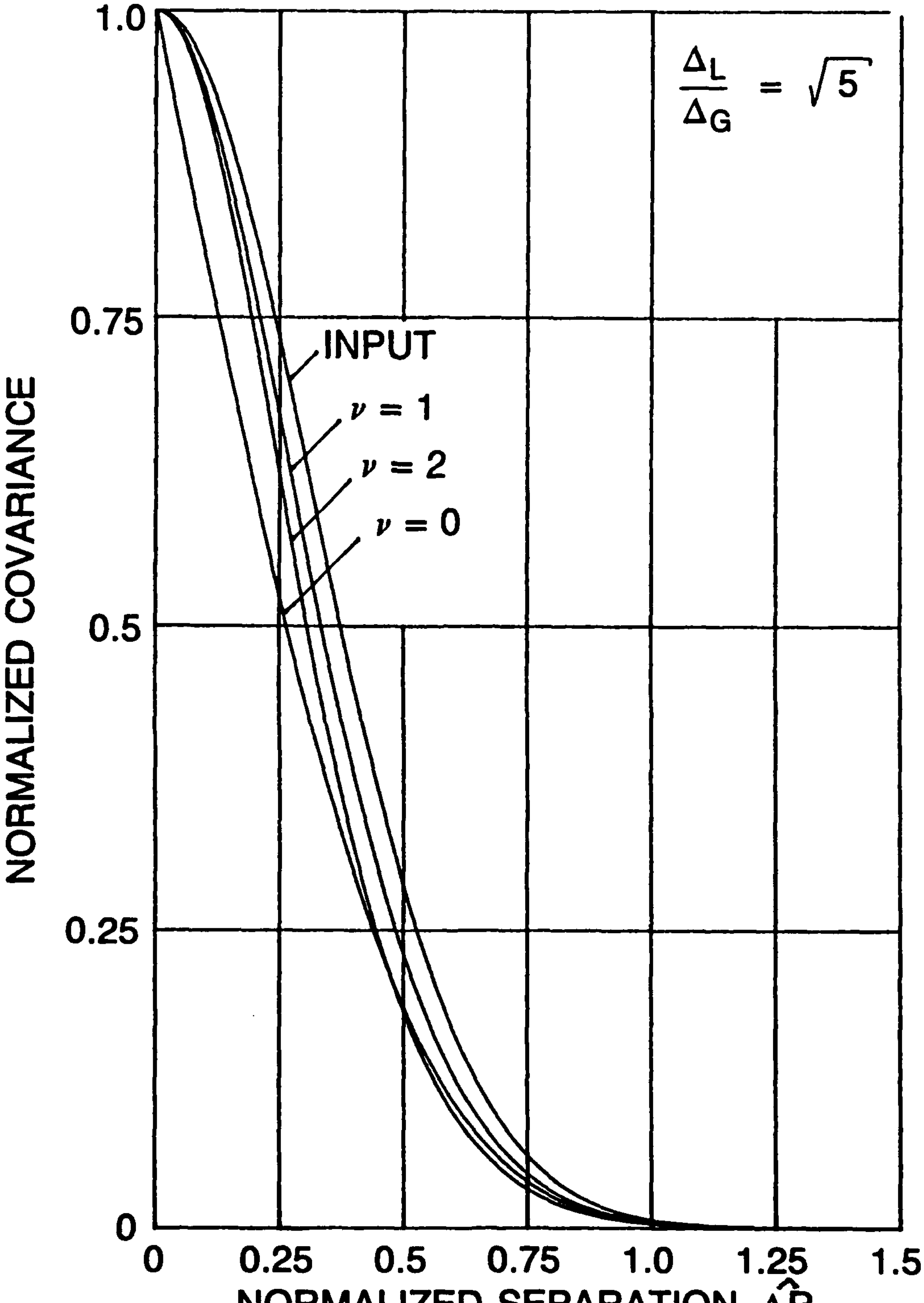

FIGURE 3.3 SPATIAL COVARIANCE (FOR $\hat{t}',\hat{t}=0$); GAUSS NOISE ONLY; CF. (2.11), (2.7b), AND APPENDIX A.2

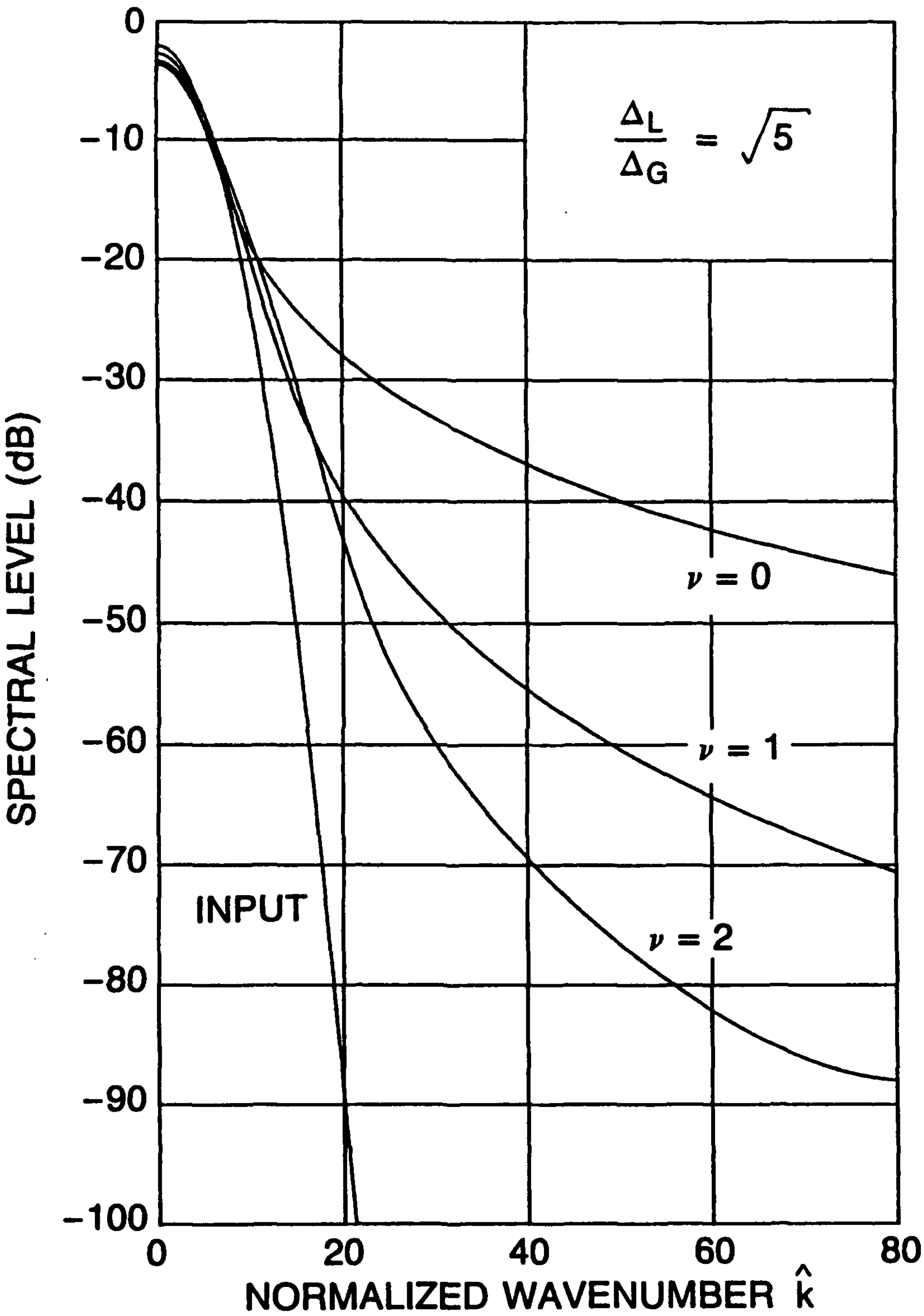

FIGURE 3.4 WAVENUMBER (INTENSITY) SPECTRUM (FOR $\hat{t}', \hat{t}=0$); GAUSS NOISE ONLY; CF. (2.35a,b) WITH (2.11), (2.7b), AND APPENDIX A.4

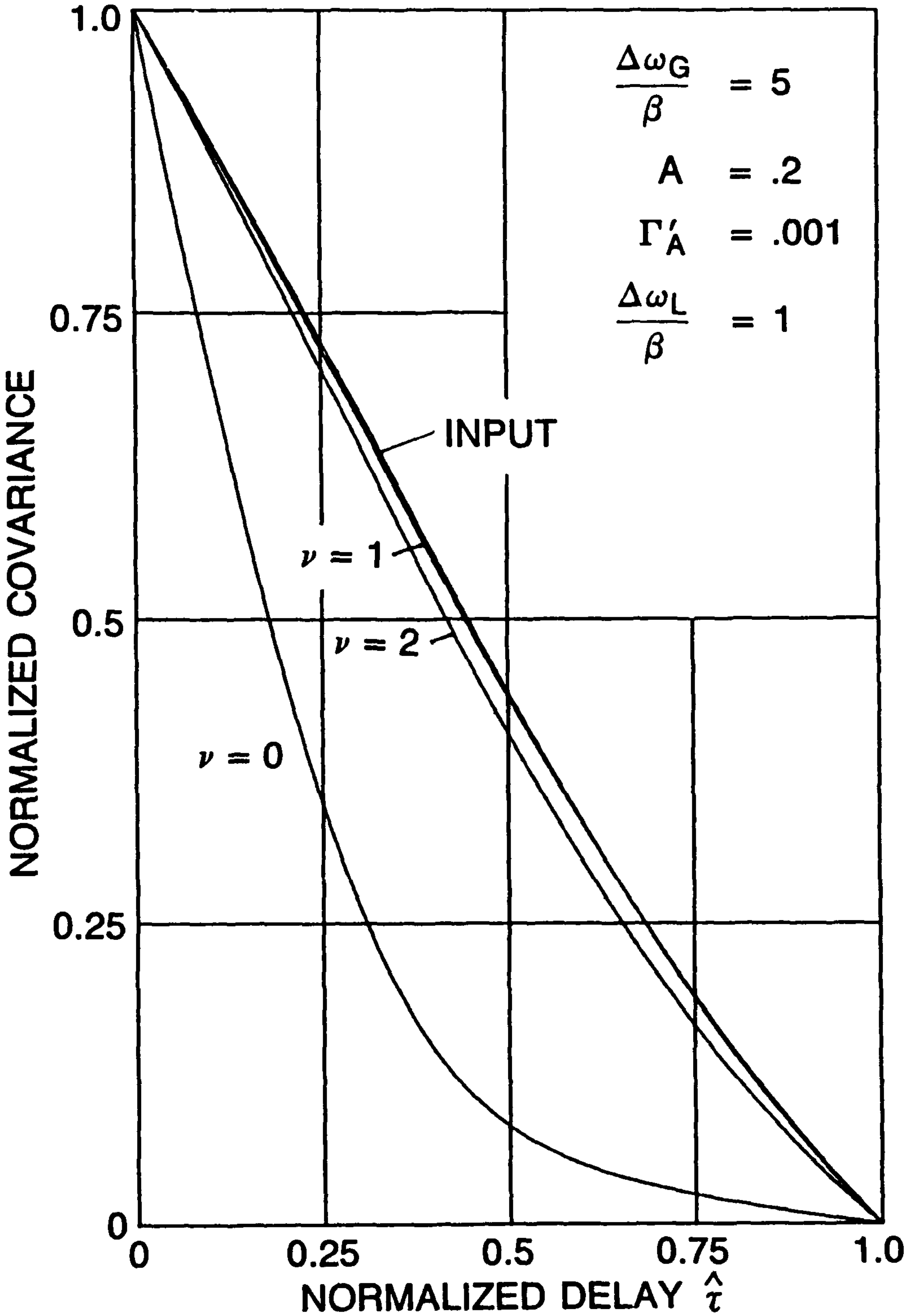

FIGURE 3.5 TEMPORAL COVARIANCE (FOR $\hat{\Delta R}=0$); CLASS A AND GAUSS NOISE; CF. (2.7)-(2.9) AND APPENDIX A.1

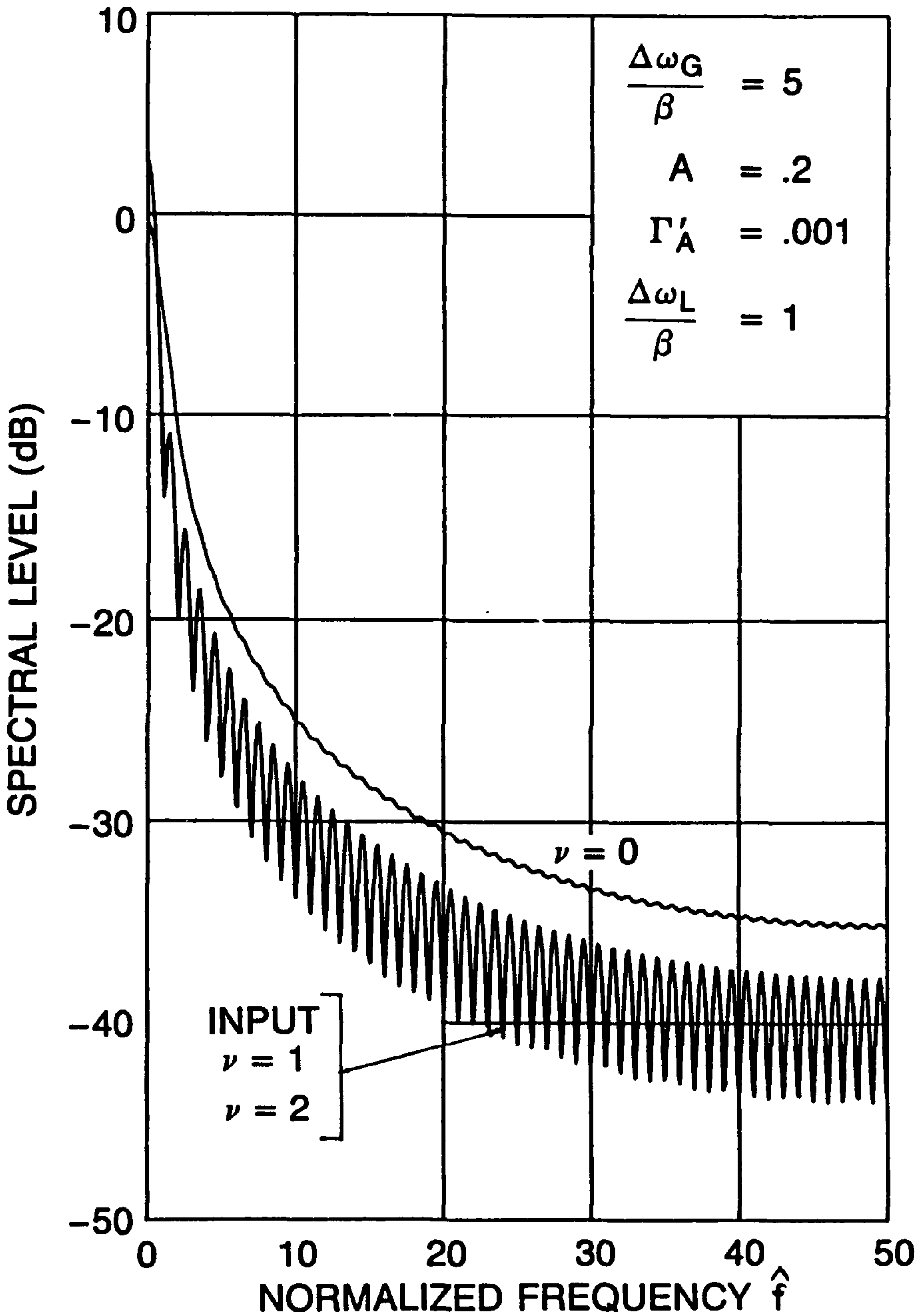

FIGURE 3.6 FREQUENCY (INTENSITY) SPECTRUM (FOR $\widehat{\Delta R}=0$); CLASS A AND GAUSS NOISE; CF. (2.7) IN (2.39) WITH APPENDIX A.3

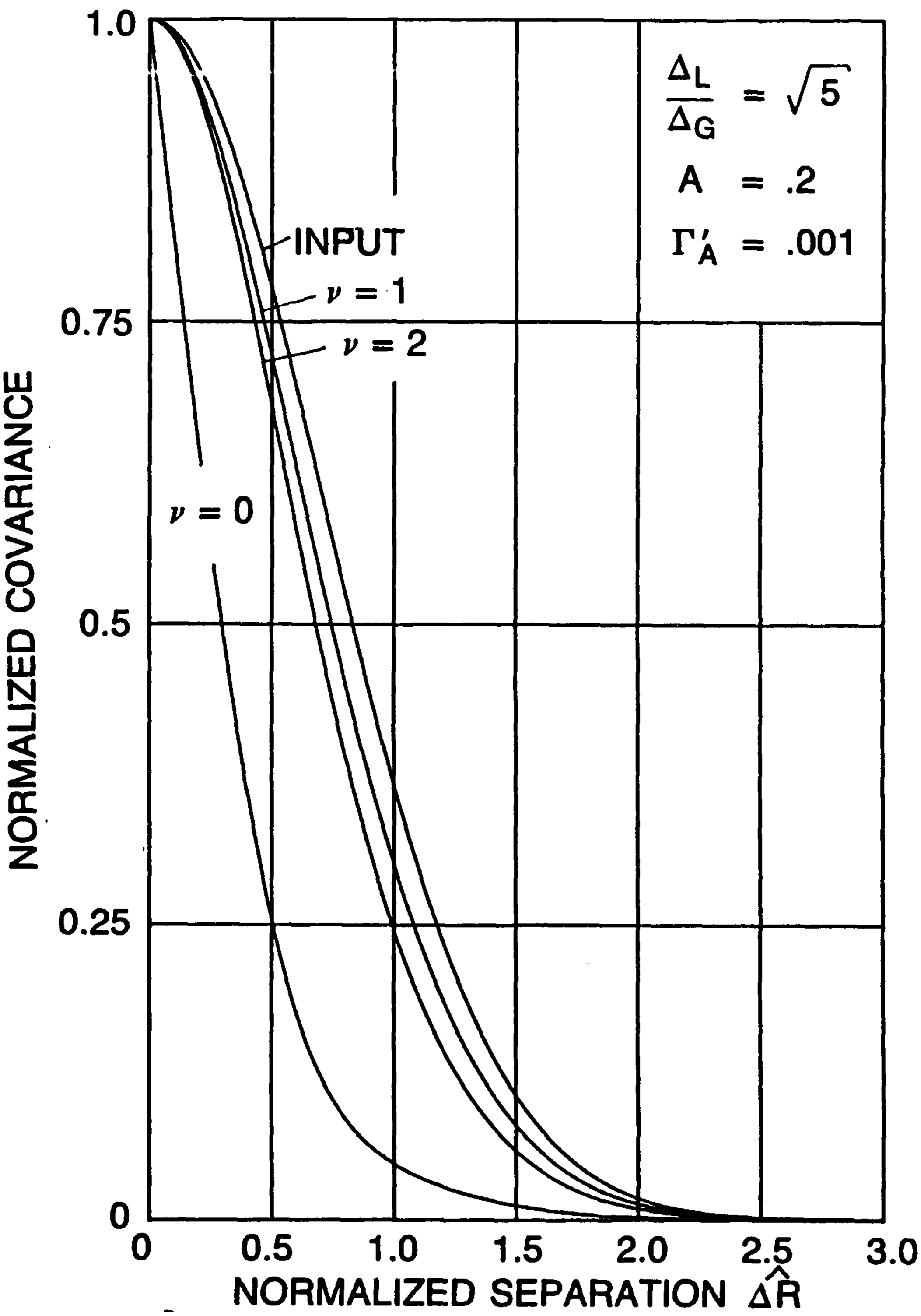

FIGURE 3.7 SPATIAL COVARIANCE (FOR $\hat{t}', \hat{t}=0$); CLASS A AND GAUSS NOISE; CF. (2.7)-(2.10) WITH APPENDIX A.2

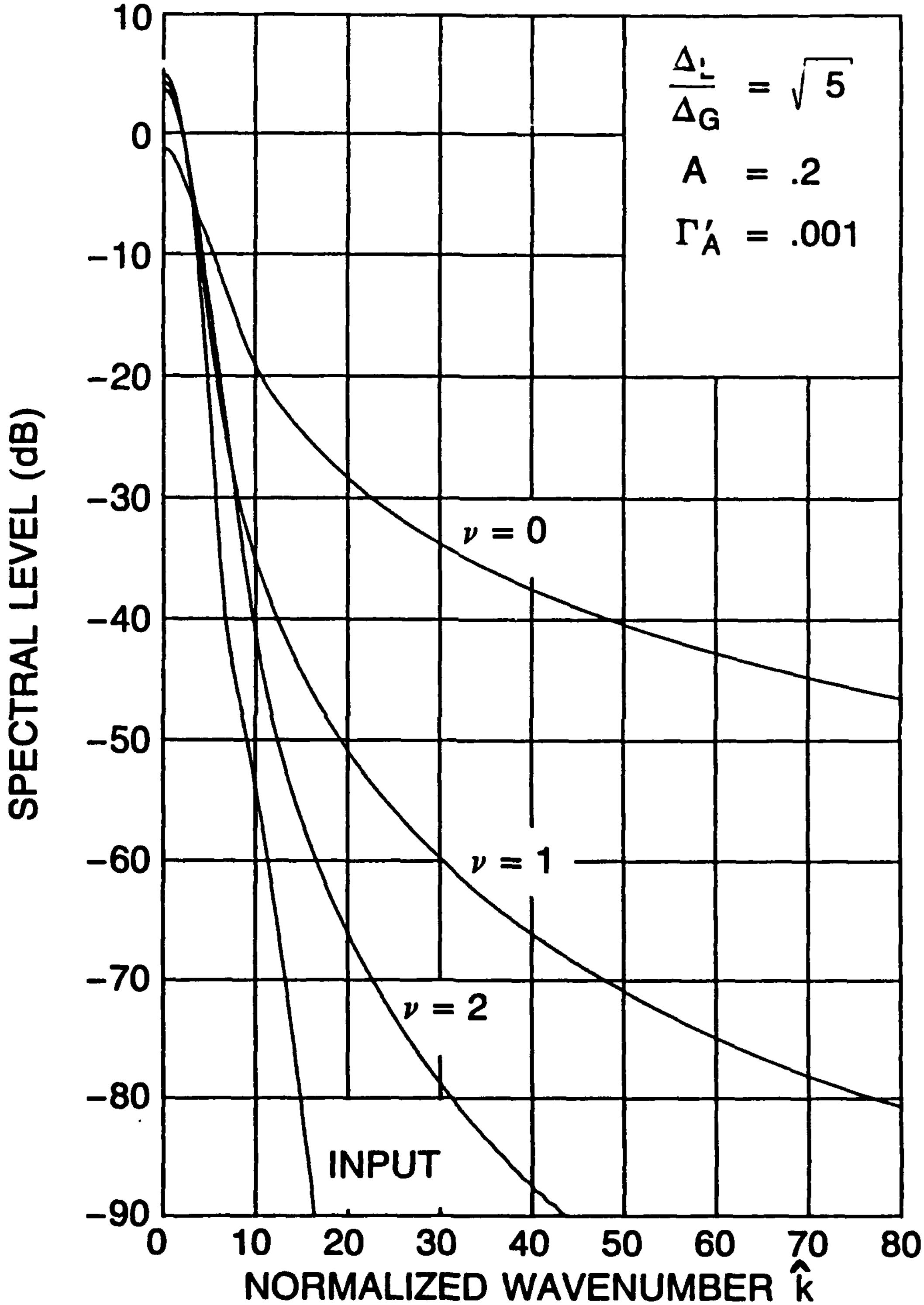

FIGURE 3.8 WAVENUMBER SPECTRUM (FOR $\hat{\tau}',\hat{\tau}=0$); CLASS A AND GAUSS NOISE; CF. (2.7)-(2.10) IN (2.38a,b) AND APPENDIX A.4

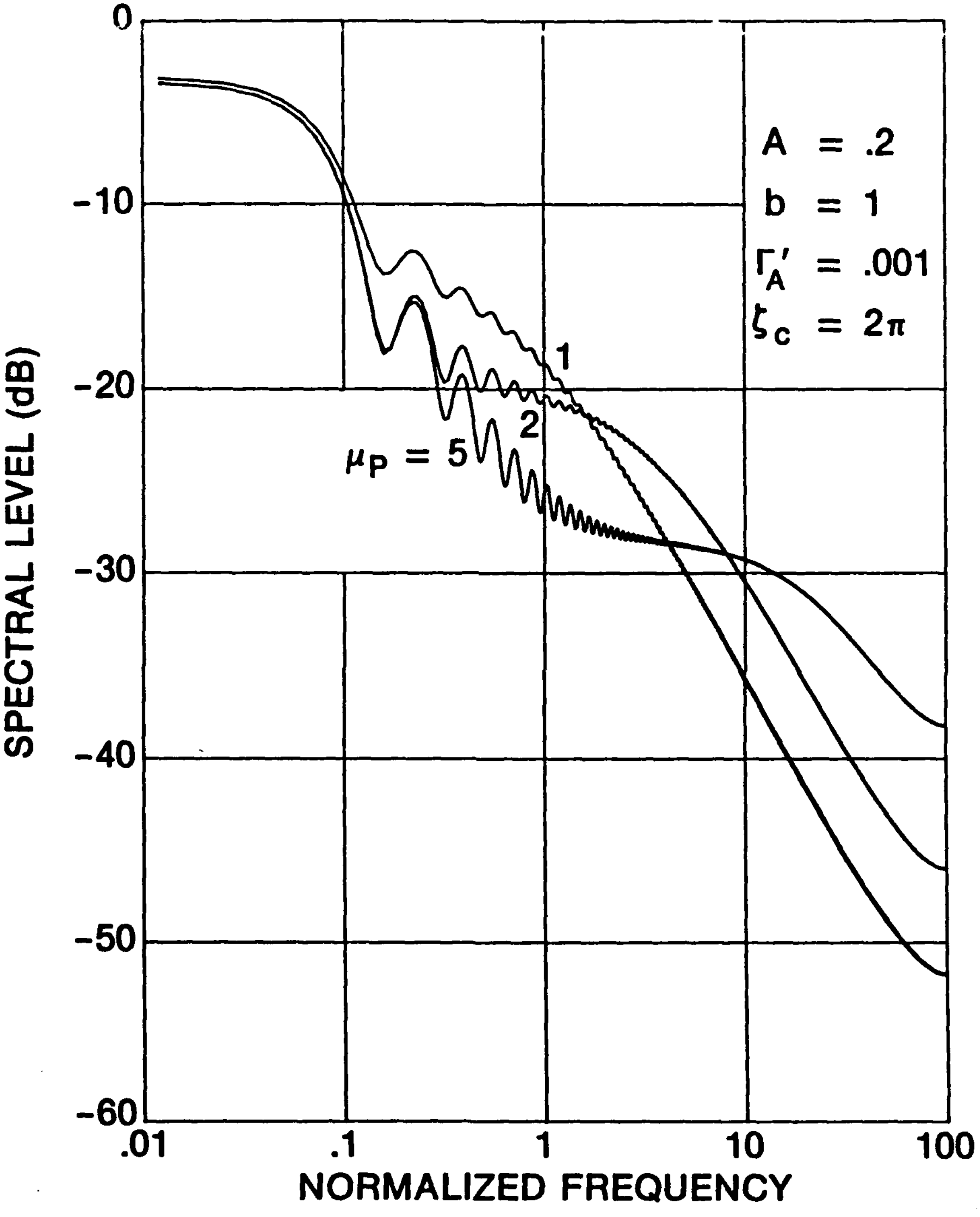

FIGURE 3.9a PHASE MODULATION (INTENSITY) SPECTRUM FOR INDEX μ_P=1,2,5, CLASS A AND GAUSS NOISE; CF. (2.50) WITH (2.44b), (2.45), (2.46) IN (2.52), AND APPENDIX A.5

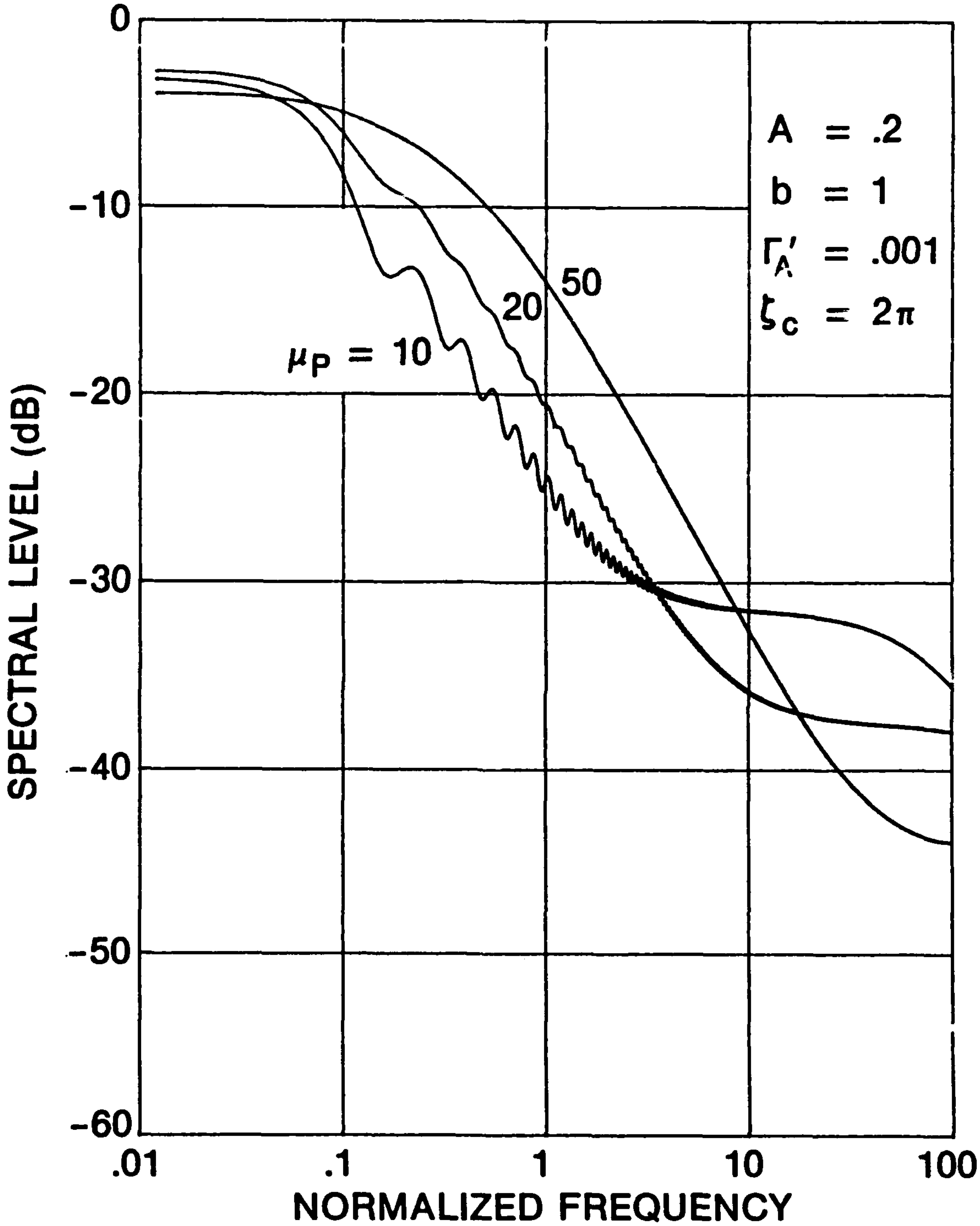

FIGURE 3.9b PHASE MODULATION (INTENSITY) SPECTRUM FOR INDEX μ_p=10,20,50, CLASS A AND GAUSS NOISE; CF. (2.50) WITH (2.44b), (2.45), (2.46) IN (2.52), AND APPENDIX A.5

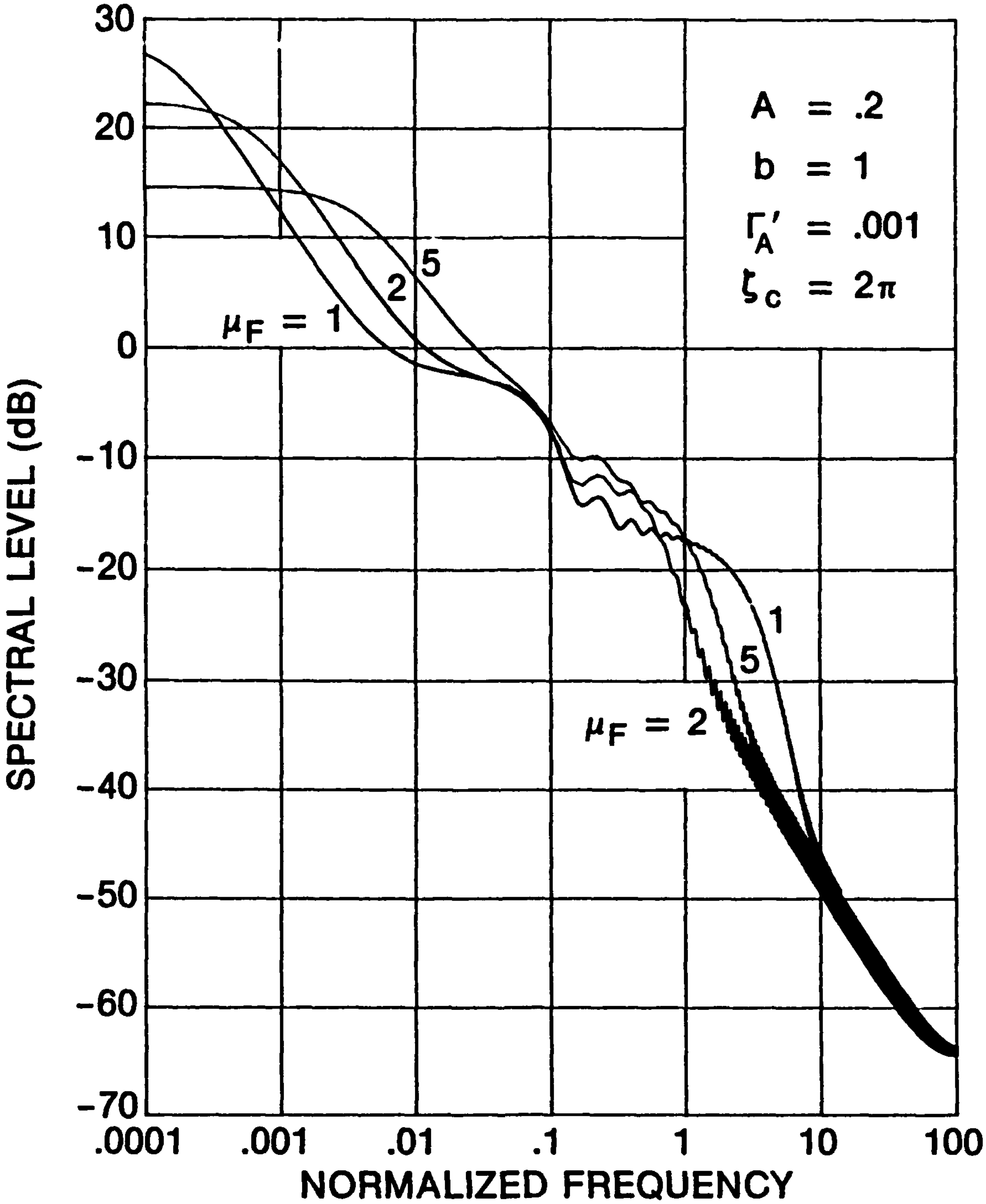

FIGURE 3.10a FREQUENCY MODULATION (INTENSITY) SPECTRUM FOR INDEX μ_F=1,2,5, CLASS A AND GAUSS NOISE; CF. (2.48) WITH (2.49), (2.44a), AND APPENDIX A.6

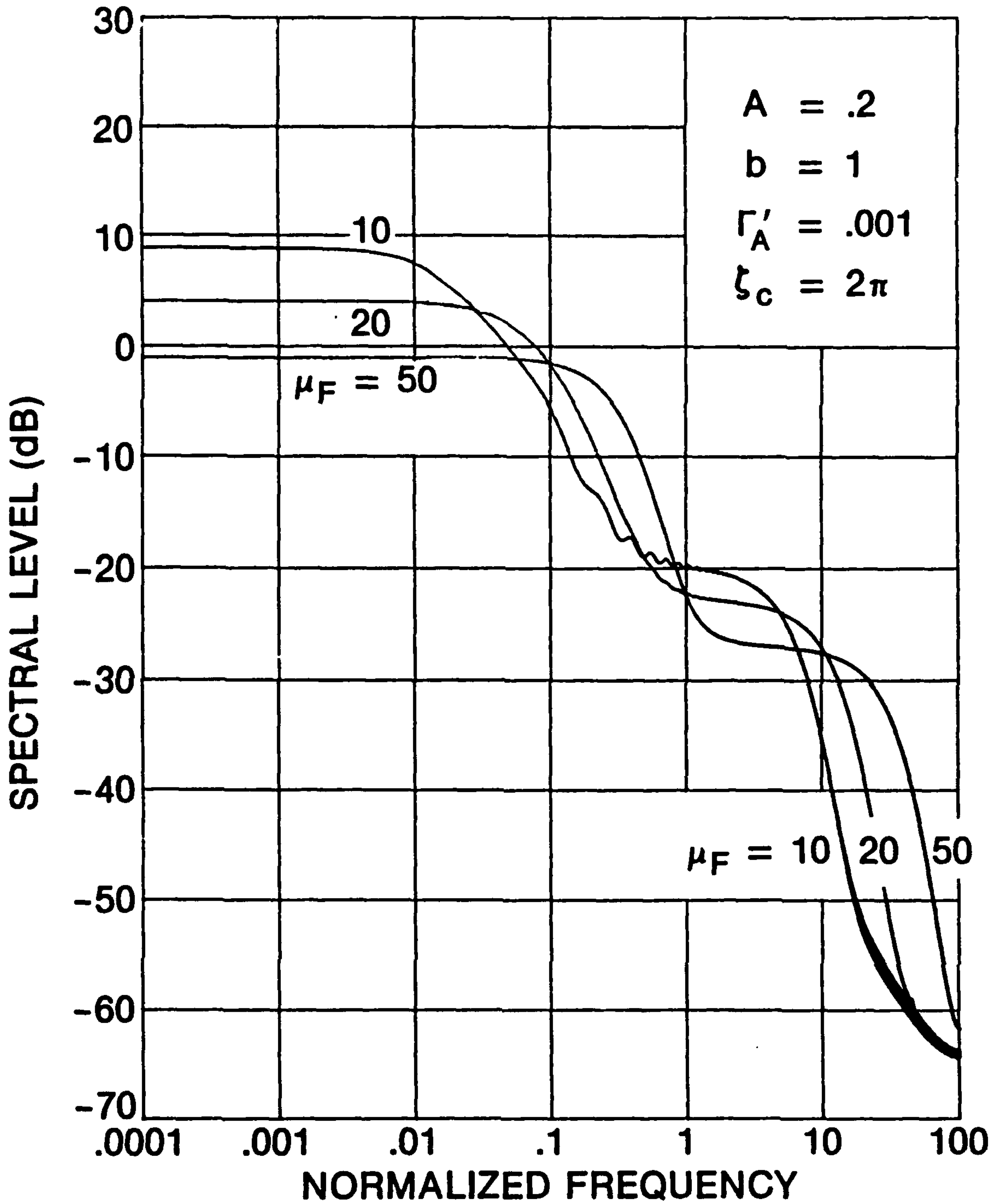

FIGURE 3.10b FREQUENCY MODULATION (INTENSITY) SPECTRUM FOR INDEX μ_F=10,20,50, CLASS A AND GAUSS NOISE; CF. (2.48) WITH (2.49), (2.44a), AND APPENDIX A.6

PART II. MATHEMATICAL AND COMPUTATIONAL PROCEDURES

4. SOME PROPERTIES OF THE COVARIANCE FUNCTION

In this section, we collect some useful relations for the covariance and auxiliary functions encountered in the numerical evaluation. These are necessary for rapid computation of the multiple series involved here and also serve as checks on the numerical procedures employed.

4.1 SIMPLIFICATION AND EVALUATION OF $B_\nu(Y)$

The function $B_\nu(Y)$ is defined by the following combination of hypergeometric functions:

$$B_\nu(Y) = \Gamma^2\left(\frac{\nu + 1}{2}\right) F\left(-\frac{\nu}{2}, -\frac{\nu}{2}; \frac{1}{2}; Y^2\right) +$$

$$+ 2\,\Gamma^2\left(\frac{\nu}{2} + 1\right) Y\,F\left(\frac{1-\nu}{2}, \frac{1-\nu}{2}; \frac{3}{2}; Y^2\right) \quad \text{for} \quad Y^2 \le 1 . \tag{4.1}$$

For the upper F function in (4.1), we have [1; (A.1.39b)]

$$\nu = 0, \quad F\left(0, 0; \frac{1}{2}; Y^2\right) = 1 ;$$

$$\nu = 1, \quad F\left(-\frac{1}{2}, -\frac{1}{2}; \frac{1}{2}; Y^2\right) = Y \arcsin(Y) + \left(1 - Y^2\right)^{\frac{1}{2}} ;$$

$$\nu = 2, \quad F\left(-1, -1; \frac{1}{2}; Y^2\right) = 1 + 2Y^2 ; \tag{4.2}$$

where arcsin is the principal value inverse sine function. On the other hand, for the latter F function in (4.1), we have [1; (A.1.39a) and (A.1.39c)]

$$\nu = 0, \quad F\left(\frac{1}{2}, \frac{1}{2}; \frac{3}{2}; Y^2\right) = \frac{\arcsin(Y)}{Y} \ ;$$

$$\nu = 1, \quad F\left(0, 0; \frac{3}{2}; Y^2\right) = 1 \ ;$$

$$\nu = 2, \ F\left(-\frac{1}{2}, -\frac{1}{2}; \frac{3}{2}; Y^2\right) = \frac{3}{4}\left(1 - Y^2\right)^{\frac{1}{2}} + \frac{1 + 2Y^2}{4Y} \arcsin(Y). \quad (4.3)$$

When these quantities are substituted in the above expression for $B_\nu(Y)$, we find the following relatively simple relations:

$$B_0(Y) = \pi + 2 \arcsin(Y) \ ,$$

$$B_1(Y) = Y \arcsin(Y) + \left(1 - Y^2\right)^{\frac{1}{2}} + \frac{\pi}{2}Y \ ,$$

$$B_2(Y) = \left(\frac{1}{2} + Y^2\right)\left(\frac{\pi}{2} + \arcsin(Y)\right) + \frac{3}{2}Y\left(1 - Y^2\right)^{\frac{1}{2}} . \qquad (4.4)$$

These three quantities can be computed simultaneously by the following very compact computer coding in BASIC:

```
Y2=Y*Y
Sq=SQR(1.-Y2)
T=ASN(Y)+1.5707963267948966
B0=T+T
B1=Y*T+Sq
B2=(.5+Y2)*T+1.5*Y*Sq                              (4.5)
```

Thus, the rather formidable expression, above, for $B_\nu(Y)$ can be evaluated by the use of just one square root and one arcsin when $\nu = 0, 1, 2$.

The following limiting values, which are obvious, are needed for various special cases:

$$\begin{aligned} B_0(0) &= \pi\ , & B_0(1) &= 2\pi\ , \\ B_1(0) &= 1\ , & B_1(1) &= \pi\ , \\ B_2(0) &= \pi/4\ , & B_2(1) &= 3\pi/2\ , \\ B_3(0) &= 1\ , & B_3(1) &= 15\pi/4\ , \\ B_4(0) &= 9\pi/16\ , & B_4(1) &= 105\pi/8\ . \end{aligned} \tag{4.6}$$

These are special cases of

$$B_\nu(0) = \Gamma^2\left(\frac{\nu + 1}{2}\right) , \tag{4.7}$$

$$B_\nu(1) = 2\ \pi^{\frac{1}{2}}\ \Gamma\left(\nu + \frac{1}{2}\right) , \tag{4.8}$$

the latter following from [10; (15.1.20)].

4.2 LIMITING VALUES OF THE COVARIANCE FUNCTION

The covariance function at normalized separation $\widehat{\Delta R}$ and delay $\hat{\tau}$ is given by (2.7) as

$$\hat{M}_y(\widehat{\Delta R},\hat{\tau}) = \exp[-A(2-\rho)] \sum_{m_1=0}^{\infty} \sum_{m_2=0}^{\infty} \frac{[A(1-\rho)]^{m_1+m_2}}{m_1!\ m_2!}$$

$$\times \sum_{n=0}^{\infty} \frac{(A\rho)^n}{n!} \left(\frac{n + m_1}{A} + \Gamma'_A\right)^{\nu/2} \left(\frac{n + m_2}{A} + \Gamma'_A\right)^{\nu/2} B_\nu(Y) , \tag{4.9}$$

where

$$\rho = \rho(\hat{\tau}) = \max\{0,\ 1 - |\hat{\tau}|\} , \tag{4.10}$$

$$Y = Y(m_1,m_2,n) = \frac{\frac{n}{A}\, k_L + \Gamma'_A\, k_G}{\left(\frac{n + m_1}{A} + \Gamma'_A\right)^{\frac{1}{2}} \left(\frac{n + m_2}{A} + \Gamma'_A\right)^{\frac{1}{2}}} , \tag{4.11}$$

$$k_L = k_L(\widehat{\Delta R},\hat{\tau}) = \exp\left[-\ \widehat{\Delta R}^2 - \frac{1}{2}\left(\frac{\Delta\omega_L}{\beta}\right)^2 \hat{\tau}^2\right] , \tag{4.12}$$

$$k_G = k_G(\widehat{\Delta R},\hat{\tau}) = \exp\left[-\ \left(\frac{\Delta_L}{\Delta_G}\right)^2 \widehat{\Delta R}^2 - \frac{1}{2}\left(\frac{\Delta\omega_G}{\beta}\right)^2 \hat{\tau}^2\right] . \tag{4.13}$$

The functions ρ, k_L, k_G can be replaced by other functional dependencies, if desired. The function $B_\nu(Y)$ has been considered earlier and considerably simplified for $\nu = 0, 1, 2$.

4.3 VALUE AT INFINITY

As $\widehat{\Delta R}$ or $\hat{\tau} \to \pm\infty$, then

$$\rho \to 0, \quad k_L \to 0, \quad k_G \to 0, \quad Y \to 0 . \tag{4.14}$$

(If $|\hat{\tau}|$ remains less than 1 as $\widehat{\Delta R}$ tends to infinity, then ρ does not approach zero; this nuance has been discussed elsewhere in this report.) Then, it follows that

$$\hat{M}_y \to \exp(-2A) \sum_{m_1=0}^{\infty} \sum_{m_2=0}^{\infty} \frac{A^{m_1+m_2}}{m_1!\ m_2!} \left(\frac{m_1}{A} + \Gamma'_A\right)^{\nu/2} \left(\frac{m_2}{A} + \Gamma'_A\right)^{\nu/2} B_\nu(0)$$

$$= B_\nu(0) \left(\exp(-A) \sum_{m=0}^{\infty} \frac{A^m}{m!} \left(\frac{m}{A} + \Gamma'_A\right)^{\nu/2}\right)^2 , \tag{4.15}$$

because the sum on n can be terminated with the n = 0 term.

The sum on m can be effected in closed form, for $\nu = 0, 2, 4$, etc., by using the following results:

$$\sum_{m=0}^{\infty} \frac{A^m}{m!} = \exp(A) , \tag{4.16}$$

$$\sum_{m=0}^{\infty} \frac{A^m}{m!}\, m = \sum_{m=1}^{\infty} \frac{A^m}{(m-1)!} = A \exp(A) \;, \tag{4.17}$$

$$\sum_{m=0}^{\infty} \frac{A^m}{m!}\, m^2 = \sum_{m=1}^{\infty} \frac{A^m}{(m-1)!} (m - 1 + 1)$$

$$= \sum_{m=2}^{\infty} \frac{A^m}{(m-2)!} + \sum_{m=1}^{\infty} \frac{A^m}{(m-1)!} = (A^2 + A) \exp(A) \;. \tag{4.18}$$

There follows

$$\hat{M}_y(\infty) = \left\{ \begin{array}{ll} \pi & \text{for } \nu = 0 \\ \frac{\pi}{4}\left(1 + \Gamma_A'\right)^2 & \text{for } \nu = 2 \\ \frac{9\pi}{16}\left[\frac{1}{A} + \left(1 + \Gamma_A'\right)^2\right]^2 & \text{for } \nu = 4 \end{array} \right\} \;. \tag{4.19}$$

The case for $\nu = 1$ requires a numerical summation, once A and Γ_A' are specified. When these limiting values are subtracted from the correlation function, we obtain the covariance function.

4.4 VALUE AT THE ORIGIN

For $\widehat{\Delta R} = 0$, $\hat{\tau} = 0$, then

$$\rho = 1, \quad k_L = 1, \quad k_G = 1 , \tag{4.20}$$

and

$$\hat{M}_y(0,0) = \exp(-A) \sum_{n=0}^{\infty} \frac{A^n}{n!} \left(\frac{n}{A} + \Gamma_A'\right)^{\nu} B_{\nu}(1) , \tag{4.21}$$

because the sums on m_1 and m_2 can be terminated with the zero terms, thereby also leading to $Y = 1$.

The sum on n can be accomplished in closed form, for $\nu = 0, 1, 2$, etc., by using results given earlier. There follows

$$\hat{M}_y(0,0) = \left\{\begin{array}{ll} 2\pi & \text{for } \nu = 0 \\ \pi\left(1 + \Gamma_A'\right) & \text{for } \nu = 1 \\ \frac{3}{2}\pi\left[\frac{1}{A} + \left(1 + \Gamma_A'\right)^2\right] & \text{for } \nu = 2 \end{array}\right\} . \tag{4.22}$$

PART III. APPENDICES AND PROGRAMS

APPENDIX A.1 – EVALUATION OF COVARIANCE FUNCTION FOR ZERO SEPARATION ($\widehat{\Delta R} = 0$)

A program for the numerical evaluation of covariance $\hat{M}_y(\widehat{\Delta R},\hat{\tau})$ for $\widehat{\Delta R} = 0$ is contained in this appendix. Inputs required of the user are A, Γ'_A, $(\Delta\omega_L/\beta)^2$, $(\Delta\omega_G/\beta)^2$, $\delta(\hat{\tau})$, $N(\hat{\tau})$, in lines 20 - 70. Since we are generally interested in values of A less than 1, the series for $\hat{M}_y$ in (4.9) will not have to be taken to very large values of m_1, m_2, n; accordingly, the values of $\{A^k/k!\}$ are tabulated once in lines 260 - 300 with a tolerance of 1E-10 set in line 80.

The values of the covariance at infinity, as given by (4.19), are computed and subtracted in lines 220 - 240 and 400 - 420; this is in anticipation of taking a Fourier transform of a covariance function which decays to zero for large arguments $\widehat{\Delta R}$.

The functions $B_\nu(Y)$ and $\hat{M}_y(\widehat{\Delta R},\hat{\tau})$ are available in the two subroutines starting at lines 1010 and 1120, respectively. The latter subroutine actually calculates the covariance at general nonzero values of both $\widehat{\Delta R}$ and $\hat{\tau}$, although we only employ it for $\widehat{\Delta R} = 0$ in this appendix; see lines 10 and 380. Also, for $\widehat{\Delta R} = 0$, the parameter Lg2 = $(\Delta_L/\Delta_G)^2$ is not relevant and, hence, is entered as zero in line 380.

The exponential Gaussian forms for k_L and k_G are used in lines 1200 and 1210, while the triangular form for ρ is entered in line 1240. Any of these can be replaced, if desired, by forms more appropriate to the user.

The program is written in BASIC for the Hewlett Packard 9000 Computer Model 520. The designation DOUBLE denotes integer variables, not double precision. The output from the program is stored in data files AOT0, AOT1, AOT2, for $\nu = 0, 1, 2$, respectively.

```
10   Rc=0.                          !  DelR^
20   A=.2                           !  A(subA)
30   Gp=.001                        !  GAMMA'(subA)
40   Wlb2=1.                        !  (DelW(subL)/Beta)^2
50   Wgb2=25.                       !  (DelW(subG)/Beta)^2
60   Dtc=.01                        !  INCREMENT IN Tau^
70   Ntc=200                        !  NUMBER OF Tau^ VALUES
80   Tolerance=1.E-10
90   COM Af(0:40),C(0:80),Sq(0:80)
100  COM DOUBLE J                   !  INTEGER
110  DIM Kag(200),Tc(0:200),F0(0:200),F1(0:200),F2(0:200)
120  DOUBLE Ntc,K                   !  INTEGERS
130  FOR K=0 TO Ntc
140  Tc=K*Dtc                       !  Tau^
150  Rho=MAX(0.,1.-ABS(Tc))         !  Rho
160  T2=.5*Tc*Tc
170  Kl=EXP(-Wlb2*T2)
180  Kg=EXP(-Wgb2*T2)
190  Kag(K)=(Rho*Kl+Gp*Kg)/(1.+Gp)     !  INPUT COVARIANCE
200  NEXT K
210  A1=1./A                        !  A>0 REQUIRED
220  F0inf=PI
230  F1inf=FNF1inf(A,Gp)
240  F2inf=.25*PI*(1.+Gp)*(1.+Gp)
250  Af(0)=1.
260  FOR K=1 TO 40
270  J=K
280  Af(K)=T=Af(K-1)*A/K            !  A^K/K!
290  IF T<Tolerance THEN 320
300  NEXT K
310  PRINT "40 TERMS IN Af(*)"
320  FOR K=0 TO J*2
330  C(K)=T=K*A1+Gp
340  Sq(K)=1./SQR(T)
350  NEXT K
360  FOR K=0 TO Ntc
370  Tc(K)=Tc=K*Dtc                 !  Tau^
380  CALL Myc(Rc,Tc,A,Gp,Wlb2,Wgb2,0.,F0(K),F1(K),F2(K))
390  NEXT K
400  MAT F0=F0-(F0inf)
410  MAT F1=F1-(F1inf)
420  MAT F2=F2-(F2inf)
430  MAT F0=F0/(F0(0))
440  MAT F1=F1/(F1(0))
450  MAT F2=F2/(F2(0))
460  PRINT "INFINITY:";F0inf;F1inf;F2inf
470  PRINT "MINIMA:  ";MIN(F0(*));MIN(F1(*));MIN(F2(*))
480  PRINT "AT Ntc:  ";F0(Ntc);F1(Ntc);F2(Ntc)
490  CREATE DATA "AIT1",8
500  ASSIGN #1 TO "AIT1"
510  PRINT #1;Kag(*)
520  CREATE DATA "AOT0",8
530  ASSIGN #1 TO "AOT0"
540  PRINT #1;F0(*)
550  CREATE DATA "AOT1",8
```

```
560    ASSIGN #1 TO "AOT1"
570    PRINT #1;F1(*)
580    CREATE DATA "AOT2",8
590    ASSIGN #1 TO "AOT2"
600    PRINT #1;F2(*)
610    ASSIGN #1 TO *
620    Tcmax=Dtc*Ntc
630    GINIT 200/260
640    PLOTTER IS 505,"HPGL"
650    PRINTER IS 505
660    LIMIT PLOTTER 505,0,200,0,260
670    VIEWPORT 22,85,19,122
680    WINDOW 0.,1.,0.,1.
690       PRINT "VS5"
700    GRID .25,.25
710       PRINT "VS36"
720    PLOT Tc(*),Kag(*)
730    PENUP
740    PLOT Tc(*),F0(*)
750    PENUP
760    PLOT Tc(*),F1(*)
770    PENUP
780    PLOT Tc(*),F2(*)
790    PENUP
800    PAUSE
810    PRINTER IS CRT
820    PLOTTER 505 IS TERMINATED
830    END
840    !
850    DEF FNF1inf(A,Gp)           !  for v(=nu) = 1
860    Tol=1.E-18
870    Ag=A*Gp
880    T=1.
890    S=SQR(1.+Ag)
900    FOR M=2 TO 100
910    T=T*A/M
920    P=T*SQR(M+Ag)
930    S=S+P
940    IF P<S*Tol THEN 970
950    NEXT M
960    PRINT "100 TERMS IN FNF1inf"
970    T=Gp+A*S*S+2.*SQR(Ag)*S
980    RETURN EXP(-2.*A)*T
990    FNEND
1000   !
1010   SUB Bnu(Y,B0,B1,B2)         !  Bv(Y) for v=0,1,2
1020   IF Y>1. THEN PRINT "Y = 1 +";Y-1.
1030   IF Y>1. THEN Y=1.
1040   Y2=Y*Y
1050   Sq=SQR(1.-Y2)
1060   T=ASN(Y)+1.5707963267948966
1070   B0=T+T
1080   B1=Y*T+Sq
1090   B2=(.5+Y2)*T+1.5*Y*Sq
1100   SUBEND
1110   !
```

```
1120    SUB Myc(Rc,Tc,A,Gp,W1b2,Wgb2,Lg2,S0,S1,S2)
1130    COM Af(*),C(*),Sq(*)
1140    COM DOUBLE J                    !  INTEGER
1150    ALLOCATE Ap(0:J),Ap1(0:J)
1160    DOUBLE K,M1,M2,N,K1,K2          !  INTEGERS
1170    A1=1./A                         !  A>0 REQUIRED
1180    T2=.5*Tc*Tc
1190    R2=Rc*Rc
1200    K1=EXP(-R2-W1b2*T2)
1210    Kg=EXP(-Lg2*R2-Wgb2*T2)
1220    Ak=A1*K1
1230    Gk=Gp*Kg
1240    Rho=MAX(0.,1.-ABS(Tc))          !  Rho
1250    Rho1=1.-Rho
1260    Ap(0)=Ap1(0)=Pk=Pk1=1.
1270    FOR K=1 TO J
1280    Pk=Pk*Rho
1290    Pk1=Pk1*Rho1
1300    T=Af(K)
1310    Ap(K)=T*Pk
1320    Ap1(K)=T*Pk1
1330    NEXT K
1340    S0m1=S1m1=S2m1=0.
1350    FOR M1=0 TO J
1360    S0m2=S1m2=S2m2=0.
1370    FOR M2=0 TO J
1380    S0n=S1n=S2n=0.
1390    FOR N=0 TO J
1400    K1=N+M1
1410    K2=N+M2
1420    T=Ap(N)
1430    P=C(K1)*C(K2)
1440    Y=(N*Ak+Gk)*Sq(K1)*Sq(K2)
1450    CALL Bnu(Y,B0,B1,B2)
1460    S0n=S0n+T*B0
1470    S1n=S1n+T*SQR(P)*B1
1480    S2n=S2n+T*P*B2
1490    NEXT N
1500    T2=Ap1(M2)
1510    S0m2=S0m2+T2*S0n
1520    S1m2=S1m2+T2*S1n
1530    S2m2=S2m2+T2*S2n
1540    NEXT M2
1550    T1=Ap1(M1)
1560    S0m1=S0m1+T1*S0m2
1570    S1m1=S1m1+T1*S1m2
1580    S2m1=S2m1+T1*S2m2
1590    NEXT M1
1600    T=EXP(-A*(2.-Rho))
1610    S0=T*S0m1
1620    S1=T*S1m1
1630    S2=T*S2m1
1640    SUBEND
```

APPENDIX A.2 — EVALUATION OF COVARIANCE FUNCTION FOR ZERO DELAY ($\hat{\tau},\hat{\tau}' = 0$)

A program for the numerical evaluation of covariance $\hat{M}_y(\hat{\Delta R},\hat{\tau})$ for $\hat{\tau},\hat{\tau}' = 0$ is contained in this appendix. Inputs required of the user are A, Γ_A', $(\Delta_L/\Delta_G)^2$, $\delta(\hat{\Delta R})$, $N(\hat{\Delta R})$, in lines 20 - 60. The tolerance for terminating the triple infinite sums is set at 1E-15 in line 70. The output from the program is stored in data files AOR0, AOR1, AOR2, for ν = 0, 1, 2, respectively. Other relevant comments are made in appendix A.1.

The limit of $\hat{M}_y$ at $\hat{\Delta R} = \infty$ (when $\hat{\tau} = 0$) is given by the closed form results

$$\hat{M}_y(\infty,0) = \begin{cases} \pi & \text{for } \nu = 0 \\ 1 + \Gamma_A' & \text{for } \nu = 1 \\ \frac{\pi}{4}\left[\frac{1}{A} + \left(1 + \Gamma_A'\right)^2\right] & \text{for } \nu = 2 \end{cases} . \tag{A.2-1}$$

These values have been subtracted from $\hat{M}_y$ so that we can Bessel transform a function which tends to zero as $\hat{\Delta R} \to \infty$.

```
10    Tc=0.                             !  Tau^
20    A=.2                              !  A(subA)
30    Gp=.001                           !  GAMMA'(subA)
40    Lg2=5.                            !  (DelL/DelG)^2
50    Drc=.005                          !  INCREMENT IN DelR^
60    Nrc=900                           !  NUMBER OF DelR^ VALUES
70    Tolerance=1.E-15
80    COM Af(0:40),C(0:80),Sq(0:80)
90    COM DOUBLE J                      !  INTEGER
100   DIM Rc(0:900),Kag(0:900),F0(0:900),F1(0:900),F2(0:900)
110   DOUBLE Nrc,K                      !  INTEGERS
120   A1=1./A                           !  A>0 REQUIRED
130   F0inf=PI                                    !  LIMITS FOR
140   F1inf=1.+Gp                                 !  Rc=infinity
150   F2inf=.25*PI*((1.+Gp)*(1.+Gp)+A1)           !  AND Tc=0
160   Af(0)=1.
170   FOR K=1 TO 40
180   J=K
190   Af(K)=T=Af(K-1)*A/K               !  A^K/K!
200   IF T<Tolerance THEN 230
210   NEXT K
220   PRINT "40 TERMS IN Af(*)"
230   FOR K=0 TO J*2
240   C(K)=T=K*A1+Gp
250   Sq(K)=1./SQR(T)
260   NEXT K
```

```
270     FOR K=0 TO Nrc
280     Rc(K)=Rc=K*Drc                 !  DelR^
290     R2=Rc*Rc
300     K1=EXP(-R2)
310     Kg=EXP(-Lg2*R2)
320     Rho=MAX(0.,1.-ABS(Tc))         !  Rho
330     Kag(K)=(Rho*K1+Gp*Kg)/(1.+Gp)   !  INPUT COVARIANCE
340     CALL Myc(Rc,Tc,A,Gp,0.,0.,Lg2,F0(K),F1(K),F2(K))
350     NEXT K
360     MAT F0=F0-(F0inf)
370     MAT F1=F1-(F1inf)
380     MAT F2=F2-(F2inf)
390     MAT F0=F0/(F0(0))
400     MAT F1=F1/(F1(0))
410     MAT F2=F2/(F2(0))
420     PRINT "INFINITY:";F0inf;F1inf;F2inf
430     PRINT "MINIMA:  ";MIN(F0(*));MIN(F1(*));MIN(F2(*))
440     PRINT "AT Nrc:  ";F0(Nrc);F1(Nrc);F2(Nrc)
450     CREATE DATA "AIR1",33
460     ASSIGN #1 TO "AIR1"
470     PRINT #1;Kag(*)
480     CREATE DATA "AOR0",33
490     ASSIGN #1 TO "AOR0"
500     PRINT #1;F0(*)
510     CREATE DATA "AOR1",33
520     ASSIGN #1 TO "AOR1"
530     PRINT #1;F1(*)
540     CREATE DATA "AOR2",33
550     ASSIGN #1 TO "AOR2"
560     PRINT #1;F2(*)
570     ASSIGN #1 TO *
580     Rcmax=Drc*Nrc
590     GINIT 200/260
600     PLOTTER IS 505,"HPGL"
610     PRINTER IS 505
620     LIMIT PLOTTER 505,0,200,0,260
630     VIEWPORT 22,85,19,122
640     WINDOW 0.,3.,0.,1.
650        PRINT "VS5"
660     GRID .5,.25
670        PRINT "VS36"
680     PLOT Rc(*),Kag(*)
690     PENUP
700     PLOT Rc(*),F0(*)
710     PENUP
720     PLOT Rc(*),F1(*)
730     PENUP
740     PLOT Rc(*),F2(*)
750     PENUP
760     PAUSE
770     PRINTER IS CRT
780     PLOTTER 505 IS TERMINATED
790     END
800     !
810     SUB Bnu(Y,B0,B1,B2)            !  Bv(Y) for v=0,1,2
820     ! SEE APPENDIX A.1
900     SUBEND
910     !
920     SUB Myc(Rc,Tc,A,Gp,Wlb2,Wgb2,Lg2,S0,S1,S2)
930     ! SEE APPENDIX A.1
1440    SUBEND
```

APPENDIX A.3 – EVALUATION OF TEMPORAL INTENSITY SPECTRUM FOR ZERO SEPARATION ($\widehat{\Delta R}$ = 0)

A program for the numerical evaluation of the Fourier transform of covariance $\hat{M}_y(0,\hat{\tau}) - \hat{M}_y(\infty)$ is contained in this appendix. Inputs required of the user are listed in lines 10 - 30. The data input, AOT0 or AOT1 or AOT2, as generated by means of the program in appendix A.1, is injected by means of lines 410, 600, and 790.

In order to keep the FFT (fast Fourier transform) size, N in lines 30 and 320, at reasonable values, the data sequence is collapsed, without any loss of accuracy, according to the method given in [8; pages 7 - 8] and [9; pages 13 - 16]. The integration rule documented here is the trapezoidal rule; this procedure is very accurate and efficient and is recommended for numerical Fourier transforms.

```
 10     Ntc=200                    !  NUMBER OF Tau^ VALUES
 20     Dtc=.01                    !  INCREMENT IN Tau^
 30     N=1024                     !  SIZE OF FFT; N > Ntc REQUIRED
 40     DOUBLE Ntc,N,N4,N2,Ns      !  INTEGERS
 50     N4=N/4
 60     N2=N/2
 70     REDIM Cos(0:N4),X(0:N-1),Y(0:N-1)
 80     DIM Cos(256),X(1023),Y(1023),A(200)
 90     T=2.*PI/N
100     FOR Ns=0 TO N4
110     Cos(Ns)=COS(T*Ns)          !  QUARTER-COSINE TABLE IN Cos(*)
120     NEXT Ns
130     GINIT 200/260
140     PLOTTER IS 505,"HPGL"
150     PRINTER IS 505
160     LIMIT PLOTTER 505,0,200,0,260
170     VIEWPORT 22,85,19,122
180     WINDOW 0,N2,-5,1
190        PRINT "VS5"
200     GRID N/10,1
210        PRINT "VS36"
220     ASSIGN #1 TO "AIT1"
230     READ #1;A(*)
240     MAT X=(0.)
250     MAT Y=(0.)
260     X(0)=.5*A(0)
270     FOR Ns=1 TO Ntc-1
280     X(Ns)=A(Ns)
290     NEXT Ns
300     X(Ntc)=.5*A(Ntc)
```

```
310     MAT X=X*(Dtc*4.)
320     CALL Fft14(N,Cos(*),X(*),Y(*))
330     FOR Ns=0 TO N2
340     Ar=X(Ns)
350     IF Ar>0. THEN 380
360     PENUP
370     GOTO 390
380     PLOT Ns,LGT(Ar)
390     NEXT Ns
400     PENUP
410     ASSIGN #1 TO "AOT0"
420     READ #1;A(*)
430     MAT X=(0.)
440     MAT Y=(0.)
450     X(0)=.5*A(0)
460     FOR Ns=1 TO Ntc-1
470     X(Ns)=A(Ns)
480     NEXT Ns
490     X(Ntc)=.5*A(Ntc)
500     MAT X=X*(Dtc*4.)
510     CALL Fft14(N,Cos(*),X(*),Y(*))
520     FOR Ns=0 TO N2
530     Ar=X(Ns)
540     IF Ar>0. THEN 570
550     PENUP
560     GOTO 580
570     PLOT Ns,LGT(Ar)
580     NEXT Ns
590     PENUP
600     ASSIGN #1 TO "AOT1"
610     READ #1;A(*)
620     MAT X=(0.)
630     MAT Y=(0.)
640     X(0)=.5*A(0)
650     FOR Ns=1 TO Ntc-1
660     X(Ns)=A(Ns)
670     NEXT Ns
680     X(Ntc)=.5*A(Ntc)
690     MAT X=X*(Dtc*4.)
700     CALL Fft14(N,Cos(*),X(*),Y(*))
710     FOR Ns=0 TO N2
720     Ar=X(Ns)
730     IF Ar>0. THEN 760
740     PENUP
750     GOTO 770
760     PLOT Ns,LGT(Ar)
770     NEXT Ns
780     PENUP
790     ASSIGN #1 TO "AOT2"
800     READ #1;A(*)
810     MAT A=A/(A(0))
820     MAT X=(0.)
830     MAT Y=(0.)
```

```
840     X(0)=.5*A(0)
850     FOR Ns=1 TO Ntc-1
860     X(Ns)=A(Ns)
870     NEXT Ns
880     X(Ntc)=.5*A(Ntc)
890     MAT X=X*(Dtc*4.)
900     CALL Fft14(N,Cos(*),X(*),Y(*))
910     FOR Ns=0 TO N2
920     Ar=X(Ns)
930     IF Ar>0. THEN 960
940     PENUP
950     GOTO 970
960     PLOT Ns,LGT(Ar)
970     NEXT Ns
980     PENUP
990     PAUSE
1000    END
1010    !
1020    SUB Fft14(DOUBLE N,REAL Cos(*),X(*),Y(*)) ! N<=2^14=16384; 0 SUBS
1030    DOUBLE Log2n,N1,N2,N3,N4,J,K   !  INTEGERS < 2^31 = 2,147,483,648
1040    DOUBLE I1,I2,I3,I4,I5,I6,I7,I8,I9,I10,I11,I12,I13,I14,L(0:13)
1050    IF N=1 THEN SUBEXIT
1060    IF N>2 THEN 1140
1070    A=X(0)+X(1)
1080    X(1)=X(0)-X(1)
1090    X(0)=A
1100    A=Y(0)+Y(1)
1110    Y(1)=Y(0)-Y(1)
1120    Y(0)=A
1130    SUBEXIT
1140    A=LOG(N)/LOG(2.)
1150    Log2n=A
1160    IF ABS(A-Log2n)<1.E-8 THEN 1190
1170    PRINT "N =";N;"IS NOT A POWER OF 2; DISALLOWED."
1180    PAUSE
1190    N1=N/4
1200    N2=N1+1
1210    N3=N2+1
1220    N4=N3+N1
1230    FOR I1=1 TO Log2n
1240    I2=2^(Log2n-I1)
1250    I3=2*I2
1260    I4=N/I3
1270    FOR I5=1 TO I2
1280    I6=(I5-1)*I4+1
1290    IF I6<=N2 THEN 1330
1300    A1=-Cos(N4-I6-1)
1310    A2=-Cos(I6-N1-1)
1320    GOTO 1350
1330    A1=Cos(I6-1)
1340    A2=-Cos(N3-I6-1)
1350    FOR I7=0 TO N-I3 STEP I3
1360    I8=I7+I5-1
1370    I9=I8+I2
1380    T1=X(I8)
1390    T2=X(I9)
```

```
1400    T3=Y(I8)
1410    T4=Y(I9)
1420    A3=T1-T2
1430    A4=T3-T4
1440    X(I8)=T1+T2
1450    Y(I8)=T3+T4
1460    X(I9)=A1*A3-A2*A4
1470    Y(I9)=A1*A4+A2*A3
1480    NEXT I7
1490    NEXT I5
1500    NEXT I1
1510    I1=Log2n+1
1520    FOR I2=1 TO 14
1530    L(I2-1)=1
1540    IF I2>Log2n THEN 1560
1550    L(I2-1)=2^(I1-I2)
1560    NEXT I2
1570    K=0
1580    FOR I1=1 TO L(13)
1590    FOR I2=I1 TO L(12) STEP L(13)
1600    FOR I3=I2 TO L(11) STEP L(12)
1610    FOR I4=I3 TO L(10) STEP L(11)
1620    FOR I5=I4 TO L(9) STEP L(10)
1630    FOR I6=I5 TO L(8) STEP L(9)
1640    FOR I7=I6 TO L(7) STEP L(8)
1650    FOR I8=I7 TO L(6) STEP L(7)
1660    FOR I9=I8 TO L(5) STEP L(6)
1670    FOR I10=I9 TO L(4) STEP L(5)
1680    FOR I11=I10 TO L(3) STEP L(4)
1690    FOR I12=I11 TO L(2) STEP L(3)
1700    FOR I13=I12 TO L(1) STEP L(2)
1710    FOR I14=I13 TO L(0) STEP L(1)
1720    J=I14-1
1730    IF K>J THEN 1800
1740    A=X(K)
1750    X(K)=X(J)
1760    X(J)=A
1770    A=Y(K)
1780    Y(K)=Y(J)
1790    Y(J)=A
1800    K=K+1
1810    NEXT I14
1820    NEXT I13
1830    NEXT I12
1840    NEXT I11
1850    NEXT I10
1860    NEXT I9
1870    NEXT I8
1880    NEXT I7
1890    NEXT I6
1900    NEXT I5
1910    NEXT I4
1920    NEXT I3
1930    NEXT I2
1940    NEXT I1
1950    SUBEND
```

APPENDIX A.4 — EVALUATION OF WAVENUMBER INTENSITY SPECTRUM FOR ZERO DELAY ($\hat{\tau},\hat{\tau}' = 0$)

A program for the numerical evaluation of the zeroth-order Bessel transform of covariance $\hat{M}_y(\widehat{\Delta R},0) - \hat{M}_y(\infty)$ is contained in this appendix. Inputs required of the user are listed in lines 10 - 40 and are coupled to appendix A.2, where the data input, AOR0 or AOR1 or AOR2, was generated. The numerical Bessel transform is accomplished by means of Simpson's rule with end correction [11; pages 414 - 418], and is exceedingly accurate for the small increment, .005, in $\widehat{\Delta R}$ employed in line 30.

```
10    Dkc=.4                    !  INCREMENT IN k^
20    Nkc=200                   !  NUMBER OF k^ VALUES
30    Drc=.005                  !  INCREMENT IN DelR^
40    Nrc=900                   !  NUMBER OF DelR^ VALUES
50    DOUBLE Nrc,Nkc,I,Ns       !  INTEGERS
60    REDIM C(0:Nrc)
70    REDIM Wi(0:Nkc),W0(0:Nkc),W1(0:Nkc),W2(0:Nkc)
80    DIM C(900),Wi(200),W0(200),W1(200),W2(200)
90    ASSIGN #1 TO "AIR1"
100   READ #1;C(*)
110   FOR I=0 TO Nkc
120   Kc=I*Dkc                  !  k^
130   T=Kc*Drc
140   Se=So=0.
150   FOR Ns=1 TO Nrc-1 STEP 2
160   So=So+Ns*FNJo(T*Ns)*C(Ns)
170   NEXT Ns
180   FOR Ns=2 TO Nrc-2 STEP 2
190   Se=Se+Ns*FNJo(T*Ns)*C(Ns)
200   NEXT Ns
210   Wi(I)=C(0)+16.*So+14.*Se
220   NEXT I
230   MAT Wi=Wi*(Drc*Drc*2.*PI/15.)
240   ASSIGN #1 TO "AOR0"
250   READ #1;C(*)
260   FOR I=0 TO Nkc
270   Kc=I*Dkc
280   T=Kc*Drc
290   Se=So=0.
300   FOR Ns=1 TO Nrc-1 STEP 2
310   So=So+Ns*FNJo(T*Ns)*C(Ns)
320   NEXT Ns
330   FOR Ns=2 TO Nrc-2 STEP 2
340   Se=Se+Ns*FNJo(T*Ns)*C(Ns)
350   NEXT Ns
360   W0(I)=C(0)+16.*So+14.*Se
370   NEXT I
380   MAT W0=W0*(Drc*Drc*2.*PI/15.)
```

```
390    ASSIGN #1 TO "AOR1"
400    READ #1;C(*)
410    FOR I=0 TO Nkc
420    Kc=I*Dkc
430    T=Kc*Drc
440    Se=So=0.
450    FOR Ns=1 TO Nrc-1 STEP 2
460    So=So+Ns*FNJo(T*Ns)*C(Ns)
470    NEXT Ns
480    FOR Ns=2 TO Nrc-2 STEP 2
490    Se=Se+Ns*FNJo(T*Ns)*C(Ns)
500    NEXT Ns
510    W1(I)=C(0)+16.*So+14.*Se
520    NEXT I
530    MAT W1=W1*(Drc*Drc*2.*PI/15.)
540    ASSIGN #1 TO "AOR2"
550    READ #1;C(*)
560    ASSIGN #1 TO *
570    FOR I=0 TO Nkc
580    Kc=I*Dkc
590    T=Kc*Drc
600    Se=So=0.
610    FOR Ns=1 TO Nrc-1 STEP 2
620    So=So+Ns*FNJo(T*Ns)*C(Ns)
630    NEXT Ns
640    FOR Ns=2 TO Nrc-2 STEP 2
650    Se=Se+Ns*FNJo(T*Ns)*C(Ns)
660    NEXT Ns
670    W2(I)=C(0)+16.*So+14.*Se
680    NEXT I
690    MAT W2=W2*(Drc*Drc*2.*PI/15.)
700    GINIT 200/260
710    PLOTTER IS 505,"HPGL"
720    PRINTER IS 505
730    LIMIT PLOTTER 505,0,200,0,260
740    VIEWPORT 22,85,19,122
750    WINDOW 0,Nkc,-9,1
760       PRINT "VS5"
770    GRID 25,1
780       PRINT "VS36"
790    FOR I=0 TO Nkc
800    W=Wi(I)
810    IF W>0. THEN 840
820    PENUP
830    GOTO 850
840    PLOT I,LGT(W)
850    NEXT I
860    PENUP
```

```
870     FOR I=0 TO Nkc
880     W=W0(I)
890     IF W>0. THEN 920
900     PENUP
910     GOTO 930
920     PLOT I,LGT(W)
930     NEXT I
940     PENUP
950     FOR I=0 TO Nkc
960     W=W1(I)
970     IF W>0. THEN 1000
980     PENUP
990     GOTO 1010
1000    PLOT I,LGT(W)
1010    NEXT I
1020    PENUP
1030    FOR I=0 TO Nkc
1040    W=W2(I)
1050    IF W>0. THEN 1080
1060    PENUP
1070    GOTO 1090
1080    PLOT I,LGT(W)
1090    NEXT I
1100    PENUP
1110    PAUSE
1120    PRINTER IS CRT
1130    PLOTTER 505 IS TERMINATED
1140    END
1150    !
1160    DEF FNJo(X)          !  Jo(X) FOR ALL X
1170    Y=ABS(X)
1180    IF Y>8. THEN 1280
1190    T=Y*Y                !  HART, #5845
1200    P=2271490439.5536033-T*(5513584.5647707522-T*5292.6171303845574)
1210    P=2334489171877869.7-T*(47765559442673.588-T*(462172225031.71803-T*P))
1220    P=185962317621897804.-T*(44145829391815982.-T*P)
1230    Q=204251483.52134357+T*(494030.79491813972+T*(884.72036756175504+T))
1240    Q=2344750013658996.8+T*(15015462449769.752+T*(64398674535.133256+T*Q))
1250    Q=185962317621897733.+T*Q
1260    Jo=P/Q
1270    RETURN Jo
1280    Z=8./Y               !  HART, #6546 & 6946
1290    T=Z*Z
1300    Pn=2204.5010439651804+T*(128.67758574871419+T*.90047934748028803)
1310    Pn=8554.8225415066617+T*(8894.4375329606194+T*Pn)
1320    Pd=2214.0488519147104+T*(130.88490049992388+T)
1330    Pd=8554.8225415066628+T*(8903.8361417095954+T*Pd)
1340    Qn=13.990976865960680+T*(1.0497327982345548+T*.0093525953294O319)
1350    Qn=-37.510534954957112-T*(46.093826814625175+T*Qn)
1360    Qd=921.56697552653090+T*(74.428389741411179+T)
1370    Qd=2400.6742371172675+T*(2971.9837452084920+T*Qd)
1380    T=Y-.78539816339744828
1390    Jo=.23209479177387820*SQR(Z)*(COS(T)*Pn/Pd-SIN(T)*Z*Qn/Qd)
1400    RETURN Jo
1410    FNEND
```

APPENDIX A.5 — EVALUATION OF PHASE MODULATION INTENSITY SPECTRUM

The normalized covariance function for phase modulation is given by (2.50) in the main text, namely

$$k_o(\zeta) = \exp\Big[- \Gamma'_A\, \mu_P^2\, [1 - \exp(-\zeta)] - A[2 - \rho(\zeta)] + \qquad \text{(A.5-1)}$$
$$+ 2A\, [1 - \rho(\zeta)]\, \exp\left(-\mu_P^2/A\right) + A\, \rho(\zeta)\, \exp\left(- \frac{\mu_P^2}{A}\, [1 - \exp(-b\zeta)]\right)\Big]$$

for $\zeta \geq 0$, where ζ is the time delay and $\rho(\zeta)$ is the temporal normalized covariance of the field process. Also $\mu_P^2 = \mu_{PG}^2$. Since (A.5-1) involves an exponential of an exponential of an exponential, and because a wide range of parameter values are of interest, care must be taken in numerical evaluation of this covariance and its transform.

Observe first that

$$k_o(0) = 1 \quad \text{since } \rho(0) = 1 \,. \qquad \text{(A.5-2)}$$

Also, as delay $\zeta \to +\infty$, then $\rho \to 0$, giving

$$k_o(\infty) = \exp\left[-\Gamma'_A\, \mu_P^2 - 2A + 2A\, \exp\left(-\mu_P^2/A\right)\right] \neq 0 \,. \qquad \text{(A.5-3)}$$

The spectrum of interest is given by

$$W_o(\omega) = 4 \int_0^\infty d\zeta\, \cos(\omega\zeta)\, k_o(\zeta) \quad \text{for } \omega \geq 0 \;;\quad \omega = 2\pi f \,. \qquad \text{(A.5-4)}$$

The nonzero value of (A.5-3) at $\zeta = \infty$ leads to an impulse in spectrum $W_o(\omega)$ at $\omega = 0$. This limiting value, $k_o(\infty)$, must be subtracted from covariance (A.5-1) prior to the numerical Fourier transform indicated by (A.5-4).

For $\Gamma_A' \mu_P^2 \ll 1$, the term

$$\exp\left(- \Gamma_A' \mu_P^2 [1 - \exp(-\zeta)]\right) \tag{A.5-5}$$

approaches its limiting value at $\zeta = +\infty$ as follows:

$$\exp\left(- \Gamma_A' \mu_P^2 [1 - \exp(-\zeta)]\right) - \exp\left(- \Gamma_A' \mu_P^2\right) =$$

$$= \exp\left(- \Gamma_A' \mu_P^2\right) \left[\exp\left(\Gamma_A' \mu_P^2 \exp(-\zeta)\right) - 1\right] =$$

$$\sim \exp\left(- \Gamma_A' \mu_P^2\right) \Gamma_A' \mu_P^2 \exp(-\zeta) \ . \tag{A.5-6}$$

This is a fairly rapid decay with ζ and will not lead to numerical difficulty when $\Gamma_A' \mu_P^2 \ll 1$.

For large $b\mu_P^2/A$, the term

$$\exp\left(- \frac{\mu_P^2}{A} [1 - \exp(-b\zeta)]\right) \tag{A.5-7}$$

is very sharp near $\zeta = 0$; in fact, it is given approximately by

$$\exp\left(- \frac{\mu_P^2}{A} b\zeta\right) \quad \text{for } \zeta \text{ near } 0 \ . \tag{A.5-8}$$

Therefore, we define the sharp component of covariance $k_o(\zeta)$ as

$$k_s(\zeta) = \exp\left[- A + A \exp\left(- \frac{\mu_P^2}{A} b\zeta\right)\right] - \exp(-A) \quad \text{for all } \zeta \ . \tag{A.5-9}$$

Then

$$k_s(0) = 1 - \exp(-A) \ , \qquad k_s(\infty) = 0 \ . \tag{A.5-10}$$

Now we let

$$k_o(\zeta) = [k_o(\zeta) - k_s(\zeta)] + k_s(\zeta) =$$

$$\equiv k_f(\zeta) + k_s(\zeta) \ , \qquad \text{(A.5-11)}$$

where $k_f(\zeta)$ is a flat function near $\zeta = 0$. Then we can express the desired difference as

$$k_o(\zeta) - k_o(\infty) = [k_f(\zeta) - k_o(\infty)] + k_s(\zeta) =$$

$$\equiv k_1(\zeta) + k_s(\zeta) \ , \qquad \text{(A.5-12)}$$

where functions $k_1(\zeta)$ and $k_s(\zeta)$ both decay to 0 at $\zeta = \infty$. We now employ two separate FFTs on each of the functions in (A.5-12). The sharp component, $k_s(\zeta)$, must be sampled with a very small increment, $\Delta\zeta$, when $b\mu_p^2/A$ is large. On the other hand, the flat component

$$k_1(\zeta) = k_f(\zeta) - k_o(\infty) \qquad \text{(A.5-13)}$$

can be sampled in a coarser fashion. Finally, if $b\mu_p^2/A$ is moderate, we work directly with $k_o(\zeta) - k_o(\infty)$ without breaking it into any components.

Two programs are furnished in this appendix, one for moderate $b\mu_p^2/A$, and the other for the flat component (A.5-13) when $b\mu_p^2/A$ is large. For sake of brevity, the Fourier transform of the sharp component (A.5-9) is straightforward and is not presented. The particular covariance $\rho(\zeta)$ adopted is triangular,

$$\rho(\zeta) = 1 - \frac{|\zeta|}{\zeta_c} \quad \text{for } |\zeta| < \zeta_c \ , \quad 0 \text{ otherwise} \ , \qquad \text{(A.5-14)}$$

but can easily be replaced. The parameter ζ_c is the cutoff value of covariance $\rho(\zeta)$.

The number of samples, N, taken of the covariance, in order to perform the FFT of (A.5-4), is rather large, so as to guarantee a very small value of truncation error at the upper end of the integral, despite the small increment $\Delta\zeta$. In order to keep the FFT size, Mf, at reasonable values, the data sequence is collapsed without any loss of accuracy according to the method given in [8; pages 7 - 8] and [9; pages 13 - 16]. The trapezoidal rule is used to approximate the integral in (A.5-4), for reasons given in [8; appendix A].

```
10  ! SPECTRUM FOR PHASE MODULATION - MODERATE
20    Mup=1.                    !  MUsubP
30    Gp=.001                   !  Gamma'
40    Bs=1.                     !  b
50    A=.2                      !  A
60    Zc=2.*PI                  !  Rho(Z) = 0 for |Z|>Zc; Z=zeta
70    Delz=.005                 !  Zeta increment
80    N=60000                   !  Maximum number of samples of ko(zeta)
90    Mf=16384                  !  Size of FFT
100   DOUBLE N,Mf,Ms,Ns         !  INTEGERS
110   DIM X(16384),Y(16384),Cos(4096)
120   REDIM X(0:Mf-1),Y(0:Mf-1),Cos(0:Mf/4)
130   MAT X=(0.)
140   MAT Y=(0.)
150   T=2.*PI/Mf
160   FOR Ms=0 TO Mf/4
170   Cos(Ms)=COS(T*Ms)         !  QUARTER-COSINE TABLE
180   NEXT Ms
190   Ta=Gp*Mup*Mup
200   IF A=0. THEN 220
210   Tb=Mup*Mup/A
220   Tc=2.*A*FNExp(Tb)
230   Kinf=FNExp(Ta+2.*A-Tc)  !  CORRELATION AT INFINITY
240   COM A,Bs,Zc,Ta,Tb,Tc,Kinf
250   T=1.-Kinf
260     PRINT 0,T
270   X(0)=T*.5                 !  TRAPEZOIDAL RULE
280   FOR Ns=1 TO N
290   Corr=FNKo(Ns*Delz)        !  CORRELATION ko(zeta)
300     IF Ns<6 THEN PRINT Ns,Corr
310   IF ABS(Corr)<1.E-30 THEN 350
320   Ms=Ns MODULO Mf           !  COLLAPSING
330   X(Ms)=X(Ms)+Corr
340   NEXT Ns
350   PRINT "Final value of Corr =";Corr;"  Ns =";Ns
360   MAT X=X*(Delz*4.)
370   CALL Fft14(Mf,Cos(*),X(*),Y(*))
```

```
380    GINIT
390    PLOTTER IS "GRAPHICS"
400    GRAPHICS ON
410    WINDOW -2,2,-60,0
420    LINE TYPE 3
430    GRID 1,10
440    LINE TYPE 1
450    Delf=1./(Mf*Delz)
460    FOR Ms=1 TO Mf/2
470    F=Ms*Delf                 !  FREQUENCY
480    PLOT LGT(F),10.*LGT(X(Ms))
490    NEXT Ms
500    PENUP
510    PAUSE
520    END
530    !
540    DEF FNExp(Xminus)         !  EXP(-X) WITHOUT UNDERFLOW
550    IF Xminus>708.3 THEN RETURN 0.
560    RETURN EXP(-Xminus)
570    FNEND
580    !
590    DEF FNKo(Zeta)            !  CORRELATION ko(zeta)
600    COM A,Bs,Zc,Ta,Tb,Tc,Kinf
610    Rho=MAX(0.,1.-Zeta/Zc)  !  TRIANGULAR RHO
620    E1=Ta*(1.-FNExp(Zeta))
630    E2=Tb*(1.-FNExp(Bs*Zeta))
640    E3=A*Rho*FNExp(E2)
650    RETURN FNExp(E1+A*(2.-Rho)-Tc*(1.-Rho)-E3)-Kinf
660    FNEND
670    !
680    SUB Fft14(DOUBLE N,REAL Cos(*),X(*),Y(*)) ! N<=2^14=16384; 0 SUBS
690    ! SEE APPENDIX A.3
```

```
 10  ! SPECTRUM FOR PHASE MODULATION - FLAT COMPONENT
 20    Mup=1.                    !  MUsubP
 30    Gp=.001                   !  Gamma'
 40    Bs=1.                     !  b
 50    A=0.                      !  A
 60    Zc=2.*PI                  !  Rho(Z) = 0 for |Z|>Zc; Z=zeta
 70    Delz=.005                 !  Zeta increment
 80    N=60000                   !  Maximum number of samples of k1(zeta)
 90    Mf=16384                  !  Size of FFT
100    DOUBLE N,Mf,Ms,Ns         !  INTEGERS
110    DIM X(16384),Y(16384),Cos(4096)
120    REDIM X(0:Mf-1),Y(0:Mf-1),Cos(0:Mf/4)
130    MAT X=(0.)
140    MAT Y=(0.)
150    T=2.*PI/Mf
160    FOR Ms=0 TO Mf/4
170    Cos(Ms)=COS(T*Ms)         !  QUARTER-COSINE TABLE
180    NEXT Ms
190    Ta=Gp*Mup*Mup
200    IF A=0. THEN 220
```

```
210     Tb=Mup*Mup/A
220     Tc=2.*A*FNExp(Tb)
230       Tb=5.E55
240     Kinf=FNExp(Ta+2.*A-Tc)  !  CORRELATION AT INFINITY
250     Ea=FNExp(A)
260     Tbb=Tb*Bs
270     COM A,Bs,Zc,Ta,Tb,Tc,Kinf,Ea,Tbb
280     T=1.-Kinf-(1.-Ea)       !  SUBTRACT SHARP COMPONENT
290       PRINT 0,T
300     X(0)=T*.5               !  TRAPEZOIDAL RULE
310     FOR Ns=1 TO N
320     Corr=FNK1(Ns*Delz)      !  CORRELATION k1(zeta)
330       IF Ns<6 THEN PRINT Ns,Corr
340     IF ABS(Corr)<1.E-30 THEN 380
350     Ms=Ns MODULO Mf         !  COLLAPSING
360     X(Ms)=X(Ms)+Corr
370     NEXT Ns
380     PRINT "Final value of Corr =";Corr;"  Ns =";Ns
390     MAT X=X*(Delz*4.)
400     CALL Fft14(Mf,Cos(*),X(*),Y(*))
410     GINIT
420     PLOTTER IS "GRAPHICS"
430     GRAPHICS ON
440     WINDOW -2,2,-60,0
450     LINE TYPE 3
460     GRID 1,10
470     LINE TYPE 1
480     Delf=1./(Mf*Delz)
490     FOR Ms=1 TO Mf/2
500     F=Ms*Delf               !  FREQUENCY
510     T=X(Ms)
520     IF T>0. THEN 550
530     PENUP
540     GOTO 560
550     PLOT LGT(F),10.*LGT(T)
560     NEXT Ms
570     PENUP
580     PAUSE
590     END
600     !
610     DEF FNExp(Xminus)       !  EXP(-X) WITHOUT UNDERFLOW
620     IF Xminus>708.3 THEN RETURN 0.
630     RETURN EXP(-Xminus)
640     FNEND
650     !
660     DEF FNK1(Zeta)          !  CORRELATION k1(zeta)
670     COM A,Bs,Zc,Ta,Tb,Tc,Kinf,Ea,Tbb
680     Rho=MAX(0.,1.-Zeta/Zc)  !  TRIANGULAR RHO
690     E1=Ta*(1.-FNExp(Zeta))
700     E2=Tb*(1.-FNExp(Bs*Zeta))
710     E3=A*Rho*FNExp(E2)
720     E4=FNExp(Tbb*Zeta)
730     Sharp=FNExp(A*(1.-E4))-Ea     !  ks(zeta)
740     RETURN FNExp(E1+A*(2.-Rho)-Tc*(1.-Rho)-E3)-Kinf-Sharp
750     FNEND
760     !
770     SUB Fft14(DOUBLE N,REAL Cos(*),X(*),Y(*)) ! N<=2^14=16384; 0 SUBS
780     ! SEE APPENDIX A.3
```

APPENDIX A.6 — EVALUATION OF FREQUENCY MODULATION INTENSITY SPECTRUM

The normalized covariance function for frequency modulation is given by (2.48) in the main text, namely

$$k_o(\zeta) = \exp\left[- \Gamma_A' \mu_F^2 [\exp(-\zeta) + \zeta - 1] - A[2 - \rho(\zeta)] + \right.$$

$$\left. + A \rho(\zeta) \exp\left(- \frac{\mu_F^2}{Ab^2} [\exp(-b\zeta) + b\zeta - 1]\right)\right] \quad \text{for } \zeta \geq 0 , \qquad (A.6\text{-}1)$$

where ζ is the time delay and $\rho(\zeta)$ is the temporal normalized covariance of the field process. Also, $\mu_F^2 = \mu_{FG}^2$ and $b = \Delta\omega_A/\Delta\omega_N$. Since (A.6-1) involves an exponential of an exponential of an exponential, and because a wide range of parameter values are of interest, care must be taken in numerical evaluation of this covariance and its transform.

Observe that

$$k_o(0) = 1 , \quad \text{because } \rho(0) = 1 . \qquad (A.6\text{-}2)$$

Also, as delay $\zeta \to +\infty$, then $\rho \to 0$, giving

$$k_o(\zeta) \sim \exp\left(- \Gamma_A' \mu_F^2 (\zeta - 1) - 2A\right) \equiv k_1(\zeta) \text{ for } \zeta > 0 . \qquad (A.6\text{-}3)$$

This term, $k_1(\zeta)$, decays slowly with ζ if $\Gamma_A' \mu_F^2 << 1$.

The spectrum of interest is given by

$$W_o(\omega) = 4 \int_0^\infty d\zeta \cos(\omega\zeta)\, k_o(\zeta) \text{ for } \omega \geq 0 ; \quad \omega = 2\pi f . \qquad (A.6\text{-}4)$$

The spectrum corresponding to the limiting component, $k_1(\zeta)$ in (A.6-3), is directly available in closed form as

$$W_1(\omega) = 4 \int_0^\infty d\zeta \cos(\omega\zeta)\, k_1(\zeta) =$$

$$= \exp\left(\Gamma'_A\, \mu_F^2 - 2A\right) \frac{4\, \Gamma'_A\, \mu_F^2}{\left(\Gamma'_A\, \mu_F^2\right)^2 + \omega^2} . \qquad \text{(A.6-5)}$$

If $\Gamma'_A\, \mu_F^2 << 1$, this latter quantity is large and very sharply peaked at $\omega = 0$; hence, this term has been subtracted out and handled separately when $\Gamma'_A\, \mu_F^2 << 1$. The residual covariance, $k_o(\zeta) - k_1(\zeta)$, then decays very rapidly with ζ and is easily handled directly by means of an FFT. This breakdown is not necessary when $\Gamma'_A\, \mu_F^2 \sim 1$ and is avoided, then, by handling $k_o(\zeta)$ directly in one FFT.

For $\mu_F^2/A >> 1$, the term

$$\exp\left(- \frac{\mu_F^2}{Ab^2} [\exp(-b\zeta) + b\zeta - 1]\right) \qquad \text{(A.6-6)}$$

inside the exponential in (A.6-1) behaves like

$$\exp\left(- \frac{\mu_F^2}{A} \frac{1}{2} \zeta^2\right) \quad \text{near } \zeta = 0 , \qquad \text{(A.6-7)}$$

where its major sharp contribution arises. For example, if $\mu_F = 50$, $A = 1$, then increment $\Delta\zeta = .005$ leads to values for (A.6-7) of

$$\exp(-0.156\, n^2) \text{ at } \zeta = n\, \Delta\zeta , \qquad \text{(A.6-8)}$$

which is adequately sampled in order to track its dominant contribution; the actual sequence of values is 1, .856, .536, .247, .083. For smaller μ_F^2/A, this sampling interval is more than adequate.

Two programs are furnished in this appendix, one each for the cases of large and small $\Gamma'_A \mu_F^2$. The particular covariance $\rho(\zeta)$ adopted is triangular,

$$\rho(\zeta) = 1 - \frac{|\zeta|}{\zeta_c} \quad \text{for } |\zeta| < \zeta_c \text{ , } \quad 0 \text{ otherwise ,} \qquad \text{(A.6-9)}$$

but can easily be replaced. The parameter ζ_c is the cutoff covariance value and is specified numerically in the examples in figures 3.9a through 3.10b.

```
 10  ! SPECTRUM FOR FREQUENCY MODULATION - LARGE Gp*Muf^2
 20    Muf=50.                   !  MUsubF
 30    Gp=.001                   !  Gamma'
 40    Bs=1.                     !  b
 50    A=.2                      !  A
 60    Zc=2.*PI                  !  Rho(Z) = 0 for |Z|>Zc; Z=zeta
 70    Delz=.005                 !  Zeta increment
 80    N=60000                   !  Maximum number of samples of ko(zeta)
 90    Mf=16384                  !  Size of FFT
100    DOUBLE N,Mf,Ms,Ns         !  INTEGERS
110    DIM X(16384),Y(16384),Cos(4096)
120    REDIM X(0:Mf-1),Y(0:Mf-1),Cos(0:Mf/4)
130    MAT X=(0.)
140    MAT Y=(0.)
150    T=2.*PI/Mf
160    FOR Ms=0 TO Mf/4
170    Cos(Ms)=COS(T*Ms)         !  QUARTER-COSINE TABLE
180    NEXT Ms
190    Ta=Gp*Muf*Muf
200    IF A=0. THEN 220
210    Tb=Muf*Muf/(A*Bs*Bs)
220    Tc=FNExp(2.*A-Ta)*Ta
230    Td=Ta*Ta
240    COM A,Bs,Zc,Ta,Tb
250    X(0)=.5                   !  TRAPEZOIDAL RULE
260    FOR Ns=1 TO N
270    Corr=FNKo(Ns*Delz)        !  CORRELATION ko(zeta)
280    IF Corr<1.E-20 THEN 320
290    Ms=Ns MODULO Mf           !  COLLAPSING
300    X(Ms)=X(Ms)+Corr
310    NEXT Ns
320    PRINT "Final value of Corr =";Corr;"  Ns =";Ns
330    MAT X=X*(Delz)
340    CALL Fft14(Mf,Cos(*),X(*),Y(*))
```

```
350     GINIT
360     PLOTTER IS "GRAPHICS"
370     GRAPHICS ON
380     WINDOW -4,2,-70,30
390     LINE TYPE 3
400     GRID 1,10
410     LINE TYPE 1
420     Delf=1./(Mf*Delz)
430     FOR Ms=1 TO Mf/2
440     F=Ms*Delf                 !  FREQUENCY
450     T=X(Ms)
460     IF T>0. THEN 490
470     PENUP
480     GOTO 500
490     PLOT LGT(F),10.*LGT(T)
500     NEXT Ms
510     PENUP
520     Add=X(0)-Tc/Td            !  ORIGIN CORRECTION
530     F=1.E-4
540     FOR Ns=1 TO 100
550     W=2.*PI*F
560     W1=Tc/(Td+W*W)
570     T=W1+Add
580     IF T>0. THEN 610
590     PENUP
600     GOTO 620
610     PLOT LGT(F),10.*LGT(W1+Add)
620     F=F*1.1                   !  FREQUENCY
630     IF F>Delf THEN 650
640     NEXT Ns
650     PENUP
660     PAUSE
670     END
680     !
690     DEF FNExp(Xminus)         !  EXP(-X) WITHOUT UNDERFLOW
700     IF Xminus>708.3 THEN RETURN 0.
710     RETURN EXP(-Xminus)
720     FNEND
730     !
740     DEF FNKo(Zeta)            !  CORRELATION ko(zeta)
750     COM A,Bs,Zc,Ta,Tb
760     E1=FNExp(Zeta)+Zeta-1.
770     T=Bs*Zeta
780     E2=FNExp(T)+T-1.
790     Rho=MAX(0.,1-Zeta/Zc)    !  TRIANGULAR RHO
800     T=Ta*E1+A*(2.-Rho)-A*Rho*FNExp(Tb*E2)
810     RETURN FNExp(T)
820     FNEND
830     !
840     SUB Fft14(DOUBLE N,REAL Cos(*),X(*),Y(*)) ! N<=2^14=16384; 0 SUBS
850     ! SEE APPENDIX A.3
```

```
 10   ! SPECTRUM FOR FREQUENCY MODULATION - SMALL Gp*Muf^2
 20     Muf=1.                      !  MUsubF
 30     Gp=.001                     !  Gamma'
 40     Bs=1.                       !  b
 50     A=.2                        !  A
 60     Zc=2.*PI                    !  Rho(Z) = 0 for |Z|>Zc; Z=zeta
 70     Delz=.005                   !  Zeta increment
 80     N=10000                     !  Maximum number of samples of ko(zeta)
 90     Mf=8192                     !  Size of FFT
100     DOUBLE N,Mf,Ms,Ns           !  INTEGERS
110     DIM X(8192),Y(8192),Cos(2048)
120     REDIM X(0:Mf-1),Y(0:Mf-1),Cos(0:Mf/4)
130     MAT X=(0.)
140     MAT Y=(0.)
150     T=2.*PI/Mf
160     FOR Ms=0 TO Mf/4
170     Cos(Ms)=COS(T*Ms)           !  QUARTER-COSINE TABLE
180     NEXT Ms
190     Ta=Gp*Muf*Muf
200     IF A=0. THEN 220
210     Tb=Muf*Muf/(A*Bs*Bs)
220     T=FNExp(2.*A-Ta)
230     Tc=T*Ta
240     Td=Ta*Ta
250     Delf=.1*Ta/(2.*PI)          !  INCREMENT IN FREQUENCY
260     COM A,Bs,Zc,Ta,Tb
270     X(0)=.5*(1.-T)              !  TRAPEZOIDAL RULE
280     FOR Ns=1 TO N
290     Corr=FNKo1(Ns*Delz)         !  CORRELATION ko(zeta)-k1(zeta)
300     IF ABS(Corr)<1.E-30 THEN 340
310     Ms=Ns MODULO Mf             !  COLLAPSING
320     X(Ms)=X(Ms)+Corr
330     NEXT Ns
340     PRINT "Final value of Corr =";Corr;"   Ns =";Ns
350     MAT X=X*(Delz)
360     CALL Fft14(Mf,Cos(*),X(*),Y(*))
```

```
370     GINIT
380     PLOTTER IS "GRAPHICS"
390     GRAPHICS ON
400     WINDOW -4,2,-70,30
410     LINE TYPE 3
420     GRID 1,10
430     LINE TYPE 1
440     FOR Ms=1 TO 2000
450     F=Ms*Delf                  !  FREQUENCY
460     W=2.*PI*F
470     W1=Tc/(Td+W*W)             !  SHARP SPECTRAL COMPONENT
480     T=Mf*Delz*F
490     Ns=INT(T)
500     Fr=T-Ns
510     W2=Fr*X(Ns+1)+(1.-Fr)*X(Ns)    !  BROAD SPECTRAL COMPONENT
520     PLOT LGT(F),10.*LGT(W1+W2)
530     NEXT Ms
540     Ns=MAX(Ns,1)
550     FOR Ms=Ns TO Mf/2
560     F=Ms/(Mf*Delz)             !  FREQUENCY
570     W=2.*PI*F
580     W1=Tc/(Td+W*W)
590     W2=X(Ms)
600     T=W1+W2
610     IF T>0. THEN 640
620     PENUP
630     GOTO 650
640     PLOT LGT(F),10.*LGT(T)
650     NEXT Ms
660     PENUP
670     PAUSE
680     END
690     !
700     DEF FNExp(Xminus)          !  EXP(-X) WITHOUT UNDERFLOW
710     IF Xminus>708.3 THEN RETURN 0.
720     RETURN EXP(-Xminus)
730     FNEND
740     !
750     DEF FNKo1(Zeta)            !  CORRELATION ko(zeta)-k1(zeta)
760     COM A,Bs,Zc,Ta,Tb
770     E1=FNExp(Zeta)+Zeta-1.
780     T=Bs*Zeta
790     E2=FNExp(T)+T-1.
800     Rho=MAX(0.,1-Zeta/Zc)      !  TRIANGULAR RHO
810     T=Ta*E1+A*(2.-Rho)-A*Rho*FNExp(Tb*E2)
820     RETURN FNExp(T)-FNExp(Ta*(Zeta-1.)+2.*A)
830     FNEND
840     !
850     SUB Fft14(DOUBLE N,REAL Cos(*),X(*),Y(*)) ! N<=2^14=16384; 0 SUBS
860     ! SEE APPENDIX A.3
```

REFERENCES

[1] D. Middleton, **An Introduction to Statistical Communication Theory**, McGraw-Hill Book Company, Inc., New York, NY, 1960. Also, Reprint Edition, Peninsula Publishing Co., P.O. Box 867, Los Altos, CA, 1987.

[2] D. Middleton, "Second-Order Non-Gaussian Probability Distributions and Their Applications to "Classical" Nonlinear Signal Processing Problems in Communication Theory," to be submitted to **IEEE Transactions on Information Theory**, 1991. (This is a considerably expanded version of [3] ff.)

[3] D. Middleton, "Second-Order Non-Gaussian Probability Distributions and Their Applications to Classical Nonlinear Processing Problems," **Proceedings of 20th Conference on Information Sciences and Systems**, pages 394-400, March 19-21, 1986, Princeton University, NJ.

[4] D. Middleton, **First- and Second-Order Gauss-Composite Processes, with Applications to Ambient and Scatter Noise**, in preparation, 1991.

[5] D. Middleton, "Canonical and Quasi-Canonical Probability Models of Class A Interference," **IEEE Transactions on Electromagnetic Compatibility**, volume EMC-25, number 2, May 1983.

[6] A. H. Nuttall, I. B. Cohen, and D. Middleton, **Performance Parameters for Quasi-Canonical Class A Non-Gaussian Noise; Source Distribution Law $\mu = 0$, Propagation Law $\gamma = 2$**, NUSC Technical Report 7715, Naval Underwater Systems Center, New London, CT, 15 June 1986.

[7] D. Middleton, "Channel Modeling and Threshold Signal Processing in Underwater Acoustics: An Analytical Overview," **IEEE Journal Oceanic Engineering**, volume OE-12, number 1, pages 4-28, January 1987.

[8] A. H. Nuttall, **Accurate Efficient Evaluation of Cumulative or Exceedance Probability Distributions Directly From Characteristic Functions**, NUSC Technical Report 7023, Naval Underwater Systems Center, New London, CT, 1 October 1983.

[9] A. H. Nuttall, "Alternative Forms and Computational Considerations for Numerical Evaluation of Cumulative Probability Distributions Directly from Characteristic Functions," **Proceedings IEEE**, volume 58, number 11, pages 1872-1873, November 1970. Also in NUSC Report Number NL-3012, Naval Underwater Systems Center, New London, CT, 12 August 1970.

[10] **Handbook of Mathematical Functions**, U. S. Department of Commerce, National Bureau of Standards, Applied Mathematics Series Number 55, U. S. Government Printing Office, Washington, DC, June 1964.

[11] C. Lanczos, **Applied Analysis**, Third Printing, Prentice-Hall, Inc., Englewood Cliffs, NJ, 1964.

[12] J. A. Mullen and D. Middleton, "The Rectification of Non-Gaussian Noise," **Quarterly Journal of Applied Mathematics**, volume XV, number 4, pages 395-419, January 1958.